

# A representation of the collisional ice break-up process in the two-moment microphysics scheme LIMA v1.0 of Meso-NH

Thomas Hoarau<sup>1</sup>, Jean-Pierre Pinty<sup>2</sup>, and Christelle Barthe<sup>1</sup>

<sup>1</sup>Laboratoire de l'Atmosphère et Cyclones, UMR 8105, CNRS/Météo-France/Université de La Réunion, St Denis, La Réunion, France

<sup>2</sup>Laboratoire d'Aérodynamique, University of Toulouse/CNRS/UPS, 14 avenue Edouard Belin, F-31400 Toulouse, France

*Correspondence to:* jean-pierre.pinty@aero.obs-mip.fr

**Abstract.** The paper describes a switchable parameterization of CIBU (Collisional Ice Break-Up), an ice multiplication process that fits in with the two-moment microphysical scheme LIMA (Liquid Ice Multiple Aerosols). The LIMA scheme with three ice types (pristine cloud ice crystals, snow-aggregates and graupel-hail) was developed in the cloud-resolving mesoscale model Meso-NH.

5 Here the CIBU process assumes that collisional break-up is mostly efficient for the small snow-aggregate class of particles with a fragile structure when hit by large ~~and~~-dense graupel particles. The increase of cloud ice number concentration depends on a prescribed number (or a random number) of fragments being produced per collision. This point is discussed and analytical expressions of the newly contributing CIBU terms in LIMA are given.

10 The scheme is run in the cloud resolving mesoscale model Meso-NH to simulate a first case of a ~~three-dimension~~ three-dimensional deep convective event with a heavy production of graupel. The consequence of dramatically changing the number of fragments produced per collision is ~~explored in particular to estimate an upper bound of the CIBU effect~~ investigated by examining the rainfall rates ~~.The case of a random number of fragments is also proposed to illustrate the consequence of~~ and the changes in small ice concentrations and mass mixing ratios. Many budgets of the ice phase are shown and the sensitivity of CIBU to the ~~uncertainty of this parameter.~~ initial IFN concentration is explored.

15 Then the scheme is tested for another deep convective case but with a varying CAPE (Convective Available Potential Energy). The results confirm the strong impact of CIBU with up to a one thousand  
20 fold increase in small ice concentrations, a reduction of the rainfall or precipitating area and an invigoration of the convection with higher cloud tops.

Finally it is concluded that the ~~assessment of CIBU certainly needs accurate laboratory experiments to check the conditions and to tune the~~ efficiency of the ~~process of~~ ice crystal fragmentation : ~~However the proposed parameterization which needs to be tuned carefully. The proposed parameterization~~  
25 ~~of CIBU~~ is easy to implement in any two-moment microphysics schemes~~-. It~~ could be used in this ~~primary~~ form to simulate deep tropical cloud systems where ~~preferential occurrence of~~ anomalously high concentrations of small ice crystals ~~are preferentially suspected to occur~~ is suspected.

## 1 Introduction

In a series of ~~paper~~papers, Yano and Phillips (2011, 2016) and Yano et al. (2016) brought the Col-  
30 lisional Ice Break-Up (hereafter CIBU) process to the fore again as a possible secondary ice pro-  
duction mechanism in clouds. Using an analytical model, they showed that the CIBU could lead to  
an explosive growth of small ice crystal concentrations. Afterwards Sullivan et al. (2017) tried to  
include CIBU in a parcel model of six species, assumed to be monodispersed here, in an attempt  
to make this finding specific. However intriguingly and in contrast to the Hallett-Mossop (hereafter  
35 H-M) ice multiplication mechanism<sup>1</sup> (Hallett and Mossop, 1974), the ~~CIBU process was overlooked~~  
~~in cloud physics. So to our knowledge, a contribution of CIBU is never accounted for in the~~ vast ma-  
jority of ~~the currently used microphysics schemes~~ microphysics schemes do not include the CIBU  
process. Yet, ~~even without absolutely incontestable clues, still missing even in recently published~~  
~~cloud data records~~<sup>2</sup>, the CIBU process is very likely to be active in the case of inhomogeneous cloud  
40 regions where ice crystals of different sizes and types are locally mixed (Hobbs and Rangno, 1985;  
Rangno and Hobbs, 2001). For instance, collisions between large dense graupel growing by riming,  
and plane vapour-grown dendrites or irregular weakly rimed assemblages are the most conceivable  
scenario for generating multiple ice debris as envisioned by Hobbs and Farber (1972) and by Griggs  
and Choulaton (1986). So a legitimate quest for a two-moment mixed-phase microphysics ~~model~~  
45 ~~such as LIMA (an acronym for Liquid, Ice, Multiple Aerosols, see Vié et al. (2016))~~ scheme, where  
number concentrations and mixing ratios of the ice crystals are predicted, is to find ways to include an  
ice-ice break-up effect and to characterize its importance, relatively to other ice generating processes  
~~like such as~~ ice heterogeneous nucleation~~, in the context of a two-moment scheme where number~~  
~~concentrations and mixing ratios of the ice crystals are predicted. At first, our~~. Our wish to introduce  
50 CIBU in a microphysics scheme ~~is essentially motivated~~ was initially motivated essentially by the  
detection of unexplained high ice water contents that sometimes largely exceed the concentration of  
ice nucleating particles (Leroy et al., 2015; Field et al., 2017; Ladino et al., 2017).

As recalled by Yano and Phillips (2011), the first few laboratory experiments dedicated to the  
study of ice collisions were conducted in the 1970s following investigations concerning the promis-  
55 ing H-M process. The pioneering work of Vardiman (1978) was a rare experimental reference show-

<sup>1</sup>H-M is based on the explosive riming of "big" droplets on graupel particles in a narrow range of temperature

<sup>2</sup>~~An inventory of the secondary ice production mechanisms is given in Table 1 of Field et al. (2017)~~

ing evidence for the mechanical fracturing of natural ice crystals. An interesting ~~issue-outcome~~ of the study was ~~to show the finding~~ that the number of fragments was dependent on the shape of the initial colliding crystal and on the momentum change following the collision. According to a concluding remark ~~of by~~ Vardiman (1978), this 'secondary' production of ice could lead to concentrations as high as 100 to 1000 times the ~~expected~~-natural concentrations of ice crystals in clouds ~~expected~~ from heterogeneous nucleation on ice freezing nuclei. Another laboratory study by Takahashi et al. (1995) also revealed a huge production of splinters after collisions between rimed and deposition-grown graupels. However the experimental set-up used there was more appropriate to very big, artificially grown crystals and to large impact velocities because as many as 400 fragments  
60 could be obtained.

For clarity, this study does not focus on cloud conditions leading to an explosive ice multiplication by mechanical break-up in ice-ice collisions (Yano and Phillips, 2011). Neither does it attempt to reformulate this process on the basis of collisional kinetic energy with many empirical parameters as proposed by Phillips et al. (2017), or earlier by Hobbs and Farber (1972) with the breaking energy,  
70 mostly applicable to "bin" microphysics schemes. Here, the goal is rather to implement an empirical but realistic parameterization of CIBU in the ~~well-suited LIMA-LIMA~~ LIMA (an acronym for Liquid, Ice, Multiple Aerosols) scheme (Vié et al., 2016) to cooperate with other microphysical processes (heterogeneous ice nucleation, droplet freezing, H-M process, etc.) to determine the concentration of small ice crystals. Our idealization of CIBU is the formation of cloud ice crystals as the result of  
75 ~~asymmetric~~-collisions between big graupel particles and small aggregates ~~followed by the erosion of the latter by the former~~ after which the graupel particles lose the mass of the aggregates. The parameterization of CIBU relies on the laboratory observations ~~of by~~ Vardiman (1978) to set limits on the number of fragments per collision. However, the large uncertainties attached to this parameter encourage us to run exploratory experiments with several fixed values and also to model the number  
80 of fragments by means of a random process with a span of two decades.

The LIMA scheme ~~is was~~ inserted in Meso-NH (Lafore et al., 1998) ~~for several sensitivity experiments~~ . Several sensitivity experiments were performed to evaluate the importance of the CIBU process and the impact of the tuning, i.e. ~~;~~ the number of fragments produced per collision. The efficiency of CIBU ~~to dramatically increase in dramatically increasing~~ the concentration of small ice  
85 crystals can be scaled by the ice ~~ice~~-number concentration from nucleation. The case of a three-dimensional continental deep convective storm, the well-known STERAO case ~~analysed-simulated~~ by Skamarock et al. (2000), provided a framework for several adjustments of the number of ice fragments. A series of experiments was then performed for the same case to see how much the CIBU process altered the precipitation and the persistence of convective plumes. The question of  
90 the number of ice nuclei necessary to initiate CIBU (Field et al., 2017; Sullivan et al., 2018) ~~is was~~ also tackled. ~~Finally~~ A second case of deep convective cloud (Weisman and Klemp, 1984) was run to confirm the impact of CIBU in a series of varying CAPE environments. The simulations showed

the invigoration of the convection when the CIBU efficiency was strong, so leading to larger cloud covers and an increase of the mean cloud top height. Finally, a conclusion is drawn on the usefulness of systematically considering importance of calibrating the parameterization of CIBU and the need to systematically include CIBU and other sources of ice multiplication in all mixed-phase two-moment ice multiplication processes in microphysics bulk schemes.

## 2 Introduction of CIBU into the LIMA scheme

### 2.1 General considerations

In contrast to the work of Yano and Phillips (2011), where large and small graupel particles fuelled the CIBU process, here we consider collisions involving two types of precipitating ice: small aggregates covering here: small ice particles growing by deposition and aggregation (aggregates including dendritic pristine ice crystals with a size larger than  $\sim 150 \mu\text{m}$  and large graupel particles. Shoeks big, massive graupel particles growing by riming. Collisions between graupel particles of different sizes are not considered because, according to Griggs and Choullarton (1986), the fragmentation of rime is very unlikely to occur in natural clouds. For the sake of simplicity and because the impact velocity of the graupel particles should be well above  $1 \text{ m s}^{-1}$  to remain in the break-up regime of the aggregates, the particle sizes are selected to enable a substantial occurrence of CIBU.

A symbolic general form of the equation describing the CIBU process can be written

$$\frac{\partial n_i}{\partial t} = \alpha n_s n_g \quad (1)$$

where  $n$  is the number concentration particle size distribution of the cloud ice (subscript "i"), the snow-aggregates ("s") and the graupel particles ("g").  $\alpha$  is the snow-aggregate-graupel collision kernel times  $\mathcal{N}_{sg}$ , the number of ice fragments produced by collision. The simplest expression of An expression for  $\alpha$ , which does not include thermal and mechanical energy effects, is

$$\alpha = \mathcal{N}_{sg} V_{sg} \frac{\pi}{4} D_g^2 \quad (2)$$

where  $V_{sg}$  is the impact velocity of a graupel particle of size  $D_g$  at the surface of the aggregate.

In Eq. 2, it is assumed that the size of the aggregate is negligible compared to  $D_g$ .  $V_{sg}$  is expressed as the difference of fall speed between the colliding graupel and the aggregate target so  $V_{sg} = (\rho_{00}/\rho_a)^{0.4} \times (c_g D_g^{d_g} - c_s D_s^{d_s})$  using the generic formula of the particle fall speeds  $V_x = (\rho_{00}/\rho_a)^{0.4} \times c_x D_x^{d_x}$  with the air density correction of Foote and du Toit (1969) due to the drag force exerted by the particles during their fall.  $\rho_{00}$  is the reference air density  $\rho_a$  at normal pressure.

As introduced above and suggested in Yano and Phillips (2011), the impact velocity  $V_{sg}$  should be such that a minimum value is guaranteed to enable CIBU. An easy way to do this is to restrict the size of the aggregates to the range [ $D_{smin}=0.2 \text{ mm}$ ,  $D_{smax}=1 \text{ mm}$ ] and to introduce a minimum size of  $D_{gmin}=2 \text{ mm}$  for the graupel particles. The reasons for these choices are discussed in the

following below. The lower bound value,  $D_{smin}$ , is an estimate that results in the collision efficiency with a graupel particle approaching unity. For  $D_s < D_{smin}$ , big crystals or aggregates stay outside the path of capture which explains the observation of bimodal ice spectra. Field (2000) reported minimum values of 150-200  $\mu\text{m}$  for  $D_{trough}$ , a critical size separating cloud ice and aggregate regimes.

130 The  $D_{smin}$  value is also consistent with an upper bound of the cloud ice crystal size distribution that results from the critical diameter of 125  $\mu\text{m}$  to convert cloud ice to snow by deposition (see Harrington et al. (1995) for the original and analytical developments and Vié et al. (2016) for the implementation in LIMA). The choice of round numbers for  $D_{smax}$  and  $D_{gmin}$  are is above all dictated by the empirical rule that  $V_{sg} > 1 \text{ m s}^{-1}$ . With the setup in LIMA which is  $[c_x, d_x] = [5.1, 0.27]$  for

135 " $x = s$ " and  $[124, 0.66]$  for " $x = g$ " in MKS units, one gets we obtain  $V_{sg} > 1.26 \text{ m s}^{-1}$  at ground level.

The number of fragments,  $\mathcal{N}_{sg}$ , is the critical parameter for ice multiplication. From scaling arguments Yano and Phillips (2011) recommended taking  $\mathcal{N}_{sg} = 50$ . Recently Yano and Phillips (2016) introduced a notion of random fluctuations into the production of fragments leading to a stochastic

140 equation of the ice crystal concentration due to the realization of a noise process for  $\alpha$  (Eq. 2). The parameterization of  $\mathcal{N}_{sg}$  as a function of collisional kinetic energy (Phillips et al., 2017) enables a differentiated treatment of the fragmentation of a variety of ice crystals. All these results start stem from Fig. 6 in Vardiman (1978) which suggests that  $\mathcal{N}_{sg}$  is a function of momentum change,  $\Delta M_g$ , after the collision. As  $\Delta M_g \sim 0.1 \text{ g cms}^{-1}$  for  $D_g = 2 \text{ mm}$ , the corresponding  $\mathcal{N}_{sg}$  lies between 10

145 (for collision with plane dendrites) and 40 (for rimed spatial crystals). These values are consistent with those found by Yano and Phillips (2011) for rimed assemblages. In conclusion, it is tempting to run both deterministic and stochastic simulations to test the sensitivity to  $\mathcal{N}_{sg}$  but in the range suggested by laboratory experiments. In the following  $\mathcal{N}_{sg}$  was set successively to 0.1 (weak effect) or alternatively one fragment per ten collisions, and to 1.0 (moderate effect) and to 10.0 or even 50

150 (strong effect) fragments per collision. Additional experiments were performed by first generating a random variable  $X$  uniformly distributed over  $[0.0, 1.0]$  and then by applying an empirical formula,  $\mathcal{N}_{sg} = 10^{2.0 \times X - 1.0}$ , to generate numbers over two decades  $[0.1, 10.0]$  of  $\mathcal{N}_{sg}$ . The randomization of  $\mathcal{N}_{sg}$  reflects the fact that the number of fragments depends on the positioning of the shock-impact, on the tip or on the body of the fragile particle, and also on the energy lost by the possible rotation

155 of the residual particle.

## 2.2 Characteristics of the LIMA microphysics scheme

The ~~microphysics~~ LIMA-LIMA microphysics scheme (Vié et al., 2016) includes a representation of the aerosols as a mixture of Cloud Condensation Nuclei (CCN) and Ice Freezing Nuclei (IFN) with an accurate budget equation (transport, activation or nucleation, scavenging by rain) for each aerosol

160 type. The CCN are selectively activated to produce the cloud droplets which grow by condensation and coalescence to produce the rain drops (Cohard and Pinty, 2000). The ice phase is more complex

as we consider ~~the~~ nucleation by deposition on ~~the IFN and the~~ insoluble IFN (black carbon and dust) and nucleation by immersion (glaciation of tagged droplets because they are formed on partially soluble CCN). ~~The homogeneous, containing an insoluble core~~. Homogeneous freezing of the droplets is possible when the temperature drops below  $-35^\circ$  C. The Hallett-Mossop mechanism generates ice crystals during the riming of the graupel and the snow-aggregates. The H-M efficiency depends sharply strongly on the temperature and on the size distribution of the droplets (Beheng, 1987). The initiation of the snow-aggregates category is the result of ~~the~~ depositional growth of large pristine crystals beyond a critical size (Harrington et al., 1995). Aggregation and riming are computed explicitly. Heavily rimed particles (graupel) can experience a dry or wet growth mode. The freezing of ~~the~~ raindrops by contact with ~~the~~ small ice crystals is leading to the frozen drops leads to frozen drops which are merged with the graupel category. The melting of ~~the~~ snow-aggregates leads to graupel and shedded shed raindrops while the graupel particles directly melt melt directly into rain. The sedimentation of all particle types is considered. The snow-aggregates and graupel particles are characterized by their mixing ratios only. The LIMA scheme assumes a strict saturation of the water vapour over the cloud droplets while the small ice crystals are subject to ~~super or undersaturated~~ super- or under-saturated conditions (no instantaneous equilibrium).

### 2.3 Representation of CIBU in the LIMA scheme

In a 2-moment bulk scheme, the zeroth order (total number concentration) and "bthb<sup>th</sup>" order (mixing ratio)<sup>2</sup> moments of the size distributions are computed. ~~So from From~~ Eqs.1 and 2 with expansion, the CIBU tendency of the number concentration of the cloud ice  $N_i$  (here in  $\# \text{ kg}^{-1}$ ) can be written as:

$$\frac{\partial N_i}{\partial t} = \frac{N_{sg}}{\rho_{dref}} \frac{\pi}{4} \left( \frac{\rho_{00}}{\rho_{dref}} \right)^{0.4} \int_{D_{smin}}^{D_{smax}} n_s(D_s) \left\{ \int_{D_{gmin}}^{\infty} D_g^2 (c_g D_g^{d_g} - c_s D_s^{d_s}) n_g(D_g) dD_g \right\} dD_s \quad (3)$$

where  $\rho_{dref}(z)$  is a reference density profile of dry air (Meso-NH is anelastic) and with a further approximation  $\rho_a = \rho_{dref}$ .

In LIMA, the size distributions follow a generalized gamma law:

$$n(D)dD = N \frac{\alpha}{\Gamma(\nu)} \lambda^{\alpha\nu} D^{\alpha\nu-1} e^{-(\lambda D)^\alpha} dD$$

where  $\alpha$  and  $\nu$  are fixed shape parameters,  $N$  is the total number concentration and  $\lambda$  is the slope parameter. With the definition of the moments  $M_x^{INC}(p; X)$  of the incomplete gamma law given in

<sup>2</sup>Ice mixing ratios are computed by integration over the size distribution of the mass of individual particles given by a mass-size relationship  $m(D) = aD^b$ , a power law with a non-integer exponent "b"

190 Appendix A, integration of Eq. 3 leads to:

$$\frac{\partial N_i}{\partial t} = \frac{N_{sg}}{\rho_{dref}} \frac{\pi}{4} \left( \frac{\rho_{00}}{\rho_{dref}} \right)^{0.4} N_s N_g \times \left\{ c_g \left( M_s^{INC}(0; D_{smin}) - M_s^{INC}(0; D_{smax}) \right) \left( M_g(2 + d_g) - M_g^{INC}(2 + d_g; D_{gmin}) \right) - c_s \left( M_s^{INC}(d_s; D_{smin}) - M_s^{INC}(d_s; D_{smax}) \right) \left( M_g(2) - M_g^{INC}(2; D_{gmin}) \right) \right\} \quad (4)$$

195

with  $N_s = C_s \lambda_s^{x_s}$  and  $N_g = C_g \lambda_g^{x_g}$ . The set of flexible parameters used in LIMA is  $C_s = 5$ ,  $C_g = 5 \times 10^5$ ,  $x_s = 1$ ,  $x_g = -0.5$ . These values were chosen to generalize the classical Marshall-Palmer law,  $n(D) = N_0 \exp(-\lambda D)$ , a degenerate form of the generalized gamma law when  $\alpha = \nu = 1$ , leading to a total concentration  $N = N_0 \lambda^{-1}$  with a fixed intercept parameter  $N_0$ .

200 Concerning the mixing ratios, the mass of the newly formed cloud ice fragments is simply taken as the product of the mean mass of the pristine ice crystals by the  $N_i$  tendency (Eq. 3). The mass loss of the aggregates after collisional break-up is equal to the mass of the ice fragments. The mass of the graupel is unchanged. The mass transfer from aggregates to small ice crystals is constrained by the mass of individual aggregates that may break up completely. This limiting mixing ratio tendency is  
205 given by:

$$\frac{\partial r_i}{\partial t} = -\frac{\partial r_s}{\partial t} = \frac{a_s}{\rho_{dref}} \frac{\pi}{4} \left( \frac{\rho_{00}}{\rho_{dref}} \right)^{0.4} \int_{D_{smin}}^{D_{smax}} D_s^{b_s} n_s(D_s) \left\{ \int_{D_{gmin}}^{\infty} D_g^2 (c_g D_g^{d_g} - c_s D_s^{d_s}) n_g(D_g) dD_g \right\} dD_s. \quad (5)$$

In the above expression the mass of an aggregate of size  $D_s$  is given by  $a_s D_s^{b_s}$  with  $a_s=0.02$  and  $b_s=1.9$  in LIMA, meaning that aggregates are quasi two-dimensional particles. After integration the mixing ratio tendencies are expressed as:

210

$$\frac{\partial r_i}{\partial t} = -\frac{\partial r_s}{\partial t} = \frac{a_s}{\rho_{dref}} \frac{\pi}{4} \left( \frac{\rho_{00}}{\rho_{dref}} \right)^{0.4} N_s N_g \times \left\{ c_g \left( M_s^{INC}(b_s; D_{smin}) - M_s^{INC}(b_s; D_{smax}) \right) \left( M_g(2 + d_g) - M_g^{INC}(2 + d_g; D_{gmin}) \right) - c_s \left( M_s^{INC}(b_s + d_s; D_{smin}) - M_s^{INC}(b_s + d_s; D_{smax}) \right) \left( M_g(2) - M_g^{INC}(2; D_{gmin}) \right) \right\} \quad (6)$$

215 This expression is independent of the number of fragments  $N_{sg}$ .

### 3 Simulation of a 3-dimensional deep convective case

The test case is illustrated by idealized numerical simulations of the 10 July 1996 thunderstorm in the Stratospheric-Tropospheric Experiment: Radiation, Aerosols, and Ozone (STRAO) experiment

(Dye et al., 2000). This case is characterized by a multicellular storm which becomes supercellular after 2 hours. The simulations were initialized with the sounding of ~~northeastern~~north eastern Colorado given in Skamarock et al. (2000) and convection was triggered by three 3K-buoyant bubbles aligned along the main diagonal of the X,Y plan in the wind axis. Meso-NH was run for 5 hours over a domain of  $320 \times 320$  with 1 km-horizontal grid spacing. There were 50 unevenly spaced vertical levels up to 23 km height. With the exception of the wind ~~component~~components advected with a  
 225 fourth-order scheme, all the fields including microphysics, were transported by an accurate, conservative, positive-definite PPM (Piecewise Parabolic Method) scheme (Colella and Woodward, 1984). There were no surface fluxes but the 3D turbulence scheme of Meso-NH was activated. Open lateral boundary conditions were imposed. The upper level damping layer of the upward moving gravity waves started above 12500 m.

230 The aerosols were initialized as for the simulated squall-line case in Vié et al. (2016). A summary is given in Table 1 for the soluble Cloud Condensation Nuclei (CCN) and for the insoluble Ice Freezing Nuclei (IFN). Homogeneous vertical profiles are assumed for the aerosols. Although the LIMA scheme incorporates size distribution parameters and differentiates between the chemical compositions of the CCN and ~~of~~ the IFN, the characteristics of the five aerosol modes are standard  
 235 for the simulations shown here, except for the sensitivity of CIBU to the initial concentration of the IFN which is explored ~~at the end of the study~~in Section 3.5.

### 3.1 Impact on precipitation

Figure 1 shows the accumulated precipitation at ground level after 4 hours of simulation for the four experiments corresponding to  $\mathcal{N}_{sg}=0.0, 0.1, 1.0$  and  $10.0$ . The highest amount of rainfall is obtained  
 240 when the CIBU process is ignored ( $\mathcal{N}_{sg}=0.0$ ) in Fig. 1a. Then, stepping up the CIBU efficiency by ~~decade~~decades from  $\mathcal{N}_{sg}=0.1$ , Fig. 1b-d clearly shows a steady reduction of precipitation and a fine scale modification of the precipitation pattern. Furthermore, Fig. 1d reveals that the spread of the precipitation field, caused by the motion of the multicellular storm, is significantly reduced when  $\mathcal{N}_{sg}=10.0$ . The results of Fig. 1 suggest empirically that a plausible range for  $\mathcal{N}_{sg}$  is be-  
 245 tween 0.1 and 10.0 fragments per collision. A value lower than 0.1 leads to a negligible effect of CIBU in the simulation, while taking  $\mathcal{N}_{sg}>10.0$  has an excessive impact on the storm rainfall (the " $\mathcal{N}_{sg}=50.0$ " case is not shown). In complement, Fig 2 shows the results of a simulation, ~~hereafter~~  
 called "RANDOM" hereafter, where  $\mathcal{N}_{sg}$  is generated by a random process as explained above but providing  $0.1 < \mathcal{N}_{sg} < 10.0$ . The perturbation caused by CIBU is noticeable in this case too but it  
 250 remains weak for the precipitation field. ~~From these~~These first 3D numerical experiments ~~it can be concluded that CIBU is clearly a disruptive process show that inclusion of CIBU can strongly modify surface precipitation~~  
~~when  $\mathcal{N}_{sg} > 10.0$  fragments per aggregate-graupel collision~~~~when taking into account the strong adverse effect on the precipitation field.~~ With, Taking  $0.1 < \mathcal{N}_{sg} < 10.0$  and ~~furthermore~~also considering  $\mathcal{N}_{sg}$  as the realization of a random process ~~it seems to be a more satis-~~

255 factory approach. Admittedly, the limit  $\mathcal{N}_{sg} \sim 10$  is more an order of magnitude but our conclusion is to recommend an upper bound value of  $\mathcal{N}_{sg}$  much lower than the former  $N=50$ , used by Yano and Phillips (2011) with their notation in the box model.

### 3.2 Changes in the microphysics

Basically, intensifying the CIBU process by increasing  $\mathcal{N}_{sg}$  ~~enhances the concentration of the cloud~~  
260 ~~ice crystals to the detriment of the mass~~ leads to higher cloud ice crystal concentrations which  
deplete the supersaturation of water vapour that would otherwise contribute to the deposition growth  
of the ~~snow-aggregate category of precipitating ice as these particles are more fragmented when~~  
 ~~$\mathcal{N}_{sg}$  is increased. However~~ snow-aggregates. However, a further effect is possible because the partial  
mass sink of the snow-aggregate particles also slows down the flux of graupel particles, which form  
265 essentially by heavy riming and conversion of the snow-aggregates. This point is now examined  
by looking at the ice in the high levels of the STERAO cells. Figures 3-5 reproduce the 10 minute  
average of the mixing ratios  $r_i$ ,  $r_s$  and  $r_g$  at 12 km height ~~of from~~ the 4 experiments  $\mathcal{N}_{sg}=0.0, 0.1, 1.0$   
and 10.0 after 4 hours. The increase of the cloud ice mixing ratio with  $\mathcal{N}_{sg}$  is clear in the area covered  
by the  $0.2 \text{ g kg}^{-1}$  isocontour in Fig. 3. Simultaneously, a slight decrease of  $r_s$ , indicating a slow  
270 erosion of the mass of the aggregates, is visible in Fig. 4. The effect on the graupel (Fig. 5) is even  
smaller but appears clearly for the case  $\mathcal{N}_{sg}=10.0$ , where less graupel is found. A last illustration  
is provided by Fig. 6, showing the number concentration of cloud ice  $N_i$  at a higher altitude of 15  
km. Again, the increase of  $N_i$  follows  $\mathcal{N}_{sg}$  with an explosive multiplication of  $N_i$  when  $\mathcal{N}_{sg}=10.0$   
( $N_i$  is well above  $1000 \text{ crystals kg}^{-1}$  of dry air in this case). Figure 7 summarizes the behaviour  
275 of  $r_i$ ,  $r_s$ ,  $r_g$  at 12 km height, and of  $N_i$  at 15 km height, for the "RANDOM" simulation. The  
results are those expected but, when comparing these results with Figs 3-6, it is not possible to find  
microphysics anomalies equivalent to the case where CIBU is not accounted for, so "RANDOM" is  
a full simulation scenario that is intermediate between  $\mathcal{N}_{sg}=1$  and  $\mathcal{N}_{sg}=10$ .

The analysis of the STERAO simulations continues by looking at the vertical profiles of micro-  
280 physics budgets. The profiles are 10 minute averages of all cloudy columns that contain at least  
 $10^{-3} \text{ g kg}^{-1}$  of condensate at any level. The column selection is updated at each time step because  
of the evolution and motion of the storm. Figure 8 shows the mixing ratio profiles in three cases:  
 $\mathcal{N}_{sg} = 0.0$ , "RANDOM" and  $\mathcal{N}_{sg} = 10.0$ . A key feature that shows up in Fig. 8a-c is the increase of  
the  $r_i$  peak value at 11 km altitude. This change is accompanied by a reduction of  $r_s$  (more visible  
285 between cases b) and c)) and by a reduction of  $r_g$  ~~which clearly,~~ which stands out at  $z=8,000 \text{ m}$ .  
The ~~final result is a decrease of the rain mixing ratio  $r_r$ , because rain is mostly fed by the melting~~  
~~of the graupel particles~~ decrease of  $r_g$ , even if graupels are passive colliders for CIBU, is the result  
of the decrease of  $r_s$  in the growth chain of the precipitating ice. The low value of the mean  $r_r$   
profile profiles, compared to the mixing ratios of the ice phase above, is explained by the fact that

290 rain is spread over fewer grid points than the ice in the anvil (the mixing ratio profiles are averaged over the same number of columns).

### 3.3 Budget of ice mixing ratios

The next step is dedicated to the microphysics tendencies (10 minute average again with the nomenclature of the processes provided in Table 3) of the ice mixing ratios in Fig. 9-11 to assess the impact 295 of the CIBU process. We do not discuss the case of the liquid phase here because the tendencies (not shown) are not very much affected by CIBU.

As expected, the tendencies of  $r_i$  (Fig. 9a-c) are the most affected by the CIBU process. The main processes standing out in Fig. 9a, when CIBU is not activated, are CEDS (Deposition-Sublimation), essentially a gain term, and AGGS (Aggregation), the main loss of  $r_i$  by aggregation with a rate of 300  $0.5 \times 10^{-3} \text{ g kg}^{-1} \text{ s}^{-1}$ . The loss of  $r_i$  by CFRZ (Drop Freezing by Contact) makes a moderate contribution as some raindrops are present in the glaciated part of the storm. ~~With Above  $z=10,000$  m, the net loss of  $r_i$  (AGGS and SEDI, the Cloud Ice Sedimentation) is balanced by the convective vertical transport (not shown). When  $\mathcal{N}_{sg}=\text{RANDOM}$ , the  $r_i$  tendencies are amplified, even with a modest contribution of  $\sim 0.2 \times 10^{-3} \text{ g kg}^{-1} \text{ s}^{-1}$  for CIBU itself. The growth of AGGS, which~~ 305 ~~doubles at 10 km height, is caused by the CIBU and by an increase in the SEDI term (Cloud Ice Sedimentation) and the presence of CIBU convection because SEDI (a loss there) is amplified in response to an increase of  $r_i$  in the upper levels.~~ The CFRZ contribution is also increased. The last case, with  $\mathcal{N}_{sg}=10$  (Fig. 9c) confirms ~~the general a further~~ increase of the rates except for CFRZ, interpreted here as a lack of raindrops.

310 The budget of the snow/aggregate mixing ratio in Fig. 10 contains many processes of equivalent importance in the range  $\pm 0.05 \times 10^{-3} \text{ g kg}^{-1} \text{ s}^{-1}$  but SEDS (Sedimentation of Snow-aggregates) dominates negatively at  ~~$z=11,000$~~   $z=11,000$  m and positively at  $z = 7,000$  m. The inclusion of CIBU (Fig. 10b-c) mostly leads to an increase of AGGS, the other processes remaining almost the same. Finally many processes contribute to the evolution of the graupel mixing ratio profiles 315 (Fig. 11). The strongest loss is in the GMLT term (Melting of graupel) that converts graupel into rain (down to  $-0.3 \times 10^{-3} \text{ g kg}^{-1} \text{ s}^{-1}$ ) while the contact freezing of the raindrops (CFRZ) reaches  $0.15 \times 10^{-3} \text{ g kg}^{-1} \text{ s}^{-1}$ . The sedimentation term SEDG (Sedimentation of Graupel) lies between  $-0.3 \times 10^{-3} \text{ g kg}^{-1} \text{ s}^{-1}$  at  $z = 10,000$  m and  $0.15 \times 10^{-3} \text{ g kg}^{-1} \text{ s}^{-1}$  at 5,000 m. Another noticeable effect is the sign change of DEPG (Growth of Graupel by Deposition,  $\pm 0.07 \times 10^{-3} \text{ g kg}^{-1} \text{ s}^{-1}$ ) 320 showing that the water vapour is super(under)saturated above(below)  $z=7,000$  m on average. The relative importance of these processes does not change very much when CIBU is increased but tendencies weaken. In summary, the impact of CIBU is modest for the microphysics mixing ratios. The increase of ice fragments in  $r_i$  is approximately compensated by an increase of AGGS (see Fig. 9 and 10).

### 325 3.4 Budget of cloud ice concentration

The next point ~~examined is~~ examines the behaviour of the cloud ice number concentration ~~according~~  
~~to as a function of~~ the strength of the CIBU process after 4 hours of simulation. Figure 12 shows  
that the altitude of the  $N_i$  peak value decreases when  $\mathcal{N}_{sg}$  increases. In the absence of CIBU ( $\mathcal{N}_{sg}$   
= 0), the ~~origin source~~ of  $N_i$  is the heterogeneous nucleation processes on insoluble IFN and on  
330 coated IFN (nucleation by immersion) which are more efficient at low temperature. ~~They provide~~  
Nucleation on IFN provides a mean peak value  $N_i = 400 \text{ kg}^{-1}$  at  $z = 11,500 \text{ m}$ . In contrast, the  
 $\mathcal{N}_{sg} = 10$  case (here scaled by  ~~$\times 0.1$~~  a factor 0.1 for plotting reasons) keeps the trace of an explosive  
production of cloud ice concentration,  $N_i = 7,250 \text{ kg}^{-1}$ , due to CIBU. The altitude of the maximum  
of  $N_i$  in this case ( $z = 10,000 \text{ m}$ ) is consistent with the location of the maximum value of the  
335  $r_s \times r_g$  product (see Fig. 8). The "RANDOM" simulation produces  $N_i = 1100 \text{ kg}^{-1}$  at  $z = 11,000$   
m, a number concentration ~~that is an order of magnitude lower~~ which is similar to that found for  
the  $\mathcal{N}_{sg} = 2$  case. Table 2 reports the peak amplitude of the  $N_i$  profiles as a function of  $\mathcal{N}_{sg}$  but  
after 3 hours of simulation, when the CIBU rate is strongly dominant. Additional cases were run to  
cover  $0.1 < \mathcal{N}_{sg} < 50$  with a logarithmic progression above  $\mathcal{N}_{sg} = 1.0$ . The CIBU enhancement factor,  
340  $\text{CIBU}_{\text{ef}}$ , is computed as  $N_i(\mathcal{N}_{sg})/N_i(\mathcal{N}_{sg} = 0) - 1$  as  $N_i(\mathcal{N}_{sg} = 0)$  stands as a baseline not affected  
by CIBU. The results ~~clearly~~ show that the growth of  $N_i$  is fast when  $\mathcal{N}_{sg}$  reaches  ~~$\sim 5.0$~~  5 ( $\text{CIBU}_{\text{ef}}$   
switches from 135% to 913% when  $\mathcal{N}_{sg}$  moves from ~~2.0 to 5.0~~ 2 to 5). Taking  $\mathcal{N}_{sg} = 50$  leads to a  
~~tremendously high  $N_i$  peak value~~ an extremely high peak value of  $N_i$ .

The  $N_i$  tendencies are the subject of Fig. 13. Many processes are involved during the temporal  
345 integration of  $N_i$ . The  $\mathcal{N}_{sg} = 0$  case confirms the importance of the heterogeneous nucleation process  
by deposition, HIND, (refer to Table 3) and, to a lesser degree, by immersion (HINC) at 8 km  
height. HIND peaks at three altitudes with two sources of IFN (Table 1). This case also reveals the  
importance of the HMG (Hallett-Mossop on Graupel,  $1.3 \text{ kg}^{-1}\text{s}^{-1}$ ) and HMS (Hallett-Mossop on  
Snow,  $0.85 \text{ kg}^{-1}\text{s}^{-1}$ ) processes. Here, we consider that H-M also operates for the snow-aggregates  
350 because this category of ice ~~is prone to light riming, like the graupel particles, in the case of water~~  
~~supercooling~~ includes lightly rimed particles that can rime further to form graupel particles. These  
processes are first compensated by AGGS (capture of cloud ice by the aggregates). There is also a  
loss of cloud ice due to CFRZ and CEDS with the full sublimation of individual cloud ice crystals  
that replenish the IFN reservoir. The sedimentation profile transports ice from cloud top ( $\text{SEDI} < 0$ )  
355 to mid-level cloud ( $\text{SEDI} > 0$ ). Then, taking  $\mathcal{N}_{sg} = \text{RANDOM}$  shows the domination of the CIBU  
process, which reaches  $2.5 \text{ kg}^{-1}\text{s}^{-1}$  at 5 km height. The enhancement of HIND at cloud top can  
also be noted. The CIBU source of ice crystals is balanced by an increase of AGGS and, above all,  
of CEDS (here CEDS represents the sublimation of the ice crystal concentration when the crystals  
are detrained in the low level of the cloud vicinity, below the anvil for instance). Finally, the  $\mathcal{N}_{sg} =$   
360 10 case demonstrates the reality of the exponential-like growth of  $N_i$  because the three main driving

terms CIBU, CEDS and AGGS are growing at a similar rate that, which is multiplied by a factor 5, approximately of approximately 5.

### 3.5 Sensitivity to the initial concentration of freezing nuclei

The purpose of the last series of experiments was to look more closely at the sensitivity of the cloud ice concentration to  $N_{IFN}$ , the initial concentration of the IFN. Numerical simulations were run with  $N_{IFN}$  decreasing by decades from  $100 \text{ dm}^{-3}$  to  $0.001 \text{ dm}^{-3}$  for each IFN mode (see Table 1). Two different cases were considered. In the first one, CIBU was activated with the RANDOM set-up while, in the second, CIBU effects were ignored. All the results are summarized in the plots of Fig. 14.

Figure 14a shows that  $N_i$  concentrations did not change very much for a wide range of  $N_{IFN}$  concentrations, which were scanned by decades. This clearly illustrates the predominance of the CIBU effect for current IFN concentrations, which disconnects  $N_i$  concentrations from the underlying abundance of IFN particles. In this vein, the small hump superimposed on all profiles at 5,000 m height reveals a residual effect of the Hallett-Mossop process. Another remarkable feature is also that a fairly low IFN concentration ( $N_{IFN} = 0.001 \text{ dm}^{-3}$ ) suffices to initiate the CIBU process and to reach  $N_i \sim 500 \text{ kg}^{-1}$ . In contrast, and in the absence of CIBU (Fig. 14b), the  $N_i$  profiles show a sensitivity to IFN nucleation that is, indeed, difficult to interpret because of the non-monotonic trend of the  $N_i$  profiles with respect to  $N_{IFN}$ . Some insight can be gained by checking the concentration of the nucleated IFN of the first IFN mode (dust particles). In Fig. 14c, the IFN profiles are rescaled (multiplication by an appropriate numbers of powers of ten) to be comparable. Here, this is equivalent to computing an IFN nucleation efficiency. The important result here is that the number of nucleated IFN evolves in close proportion to the initially available IFN concentrations, meaning that the nucleating properties of the IFN do not depend on the IFN concentration as expected. The last plot (Fig. 14d) reproduces the normalized differences of  $N_i$  profiles between twin simulations performed with CIBU and without CIBU. Even if simulations made with the same initial concentration  $N_{IFN}$ , diverge because of additional non-linear effects (vertical transport, enhanced or reduced cloud ice sink processes), the figure gives a flavour of the bulk sensitivity of CIBU to the IFN. The enhancement ratio due to CIBU remains low (less than 1 for  $N_{IFN} \sim 100 \text{ dm}^{-3}$ ) but can reach a factor of 20 at 9,000 m height in the case of moderate IFN concentration i.e.  $N_{IFN} \sim 1 \text{ dm}^{-3}$ . The behaviour of LIMA can be explained in the sense that increasing  $N_{IFN}$  too much leads to smaller pristine crystals that need a longer time to grow because the conversion to the next category of snow-aggregates is size-dependent (see Harrington et al. (1995) and Vié et al. (2016)). On the other hand, a low concentration of  $N_{IFN}$  initiates fewer snow-aggregate and thus less fewer graupel particles, so the whole CIBU efficiency is also reduced. Consequently, this study confirms the essential role of CIBU to compensate in compensating for IFN deficit when cloud ice concentrations are building up.

#### 4 Simulation of a 3-dimensional idealized supercell storm with varying atmospheric stability

The test case (referred as WK) was suggested by the idealized sounding of Weisman and Klemp (1982, 1984) where the intensity of the CAPE can be easily modified by changing a reference water vapour mixing ratio.

400 The simulation conditions were close to those of the STERAO case with the same set-up for the physics and the aerosol characteristics. The domain simulation was  $180 \times 180$  at 1 km resolution and 70 levels with a mean vertical grid spacing of 350 m. Convection was triggered by a domain-centered single 2K-buoyant air parcel of 10 km radius and 3 km height. The base of the upper level Rayleigh damper was set at 15 km above the ground.

405 Meso-NH was initialized with the analytic sounding of Weisman and Klemp (1984) with a low 2-dimensional shear. The hodograph in Fig. 15 features a three-quarter-cycle with a constant wind of  $6.4 \text{ m s}^{-1}$  (in modulus) above the height of 5 km. When running Meso-NH a constant translation speed ( $U_{trans}=5 \text{ m s}^{-1}$  and  $V_{trans}=1 \text{ m s}^{-1}$ ) was added to the wind to keep the convection well centered in the domain of simulation. As explained in Weisman and Klemp (1982), buoyancy is varied by altering the magnitude of the surface water vapour mixing ratio  $q_{v0}$  in Weisman and  
410 Klemp notation. So three water vapour profiles were defined taking  $q_{v0} = 13.5 \text{ g kg}^{-1}$ , hereafter the "Low" CAPE case of  $1970 \text{ J kg}^{-1}$ ;  $q_{v0} = 14.5 \text{ g kg}^{-1}$  as the "Mid" CAPE case of  $2400 \text{ J kg}^{-1}$ , and  $q_{v0} = 15.5 \text{ g kg}^{-1}$ , the "High" CAPE case with  $2740 \text{ J kg}^{-1}$ . Four 4h-experiments were performed for each CAPE case by changing the magnitude of  $\mathcal{N}_{sg}$ .

##### 415 4.1 Sensitivity to the mean ice concentrations

The mean concentrations of the small ice crystals between 9.5 and 10.5 km levels are plotted on a log scale in Fig. 16 after 4 hours of simulation. In addition, two CTH (Cloud Top Height) isocontours delineate the 11 km (dotted line) and 13 km (solid line) levels. The  $\mathcal{N}_{sg} = 0, \text{RANDOM}, 10$  and 50 cases, are explored for each sounding ("Low", "Mid" and "High" CAPE). In the absence of CIBU  
420 (first row in Fig. 16), the cloud ice concentrations  $N_i$  are in the range of what was simulated for the STERAO case (see Figs. 6 and 7d). The  $N_i$  peak values do not increase with the initial CAPE (Figs 16a-b) but the area of  $\text{CTH} > 11 \text{ km}$  is larger in the "Mid CAPE" case. The "High CAPE" case is a little more difficult to analyse because of an earlier development of the convection, spreading out ahead of the main system, showing up in the "Low" and "Mid" CAPE cases. However, the  $N_i$  peak  
425 values of the "High" CAPE case are in the range of the "Low" CAPE case, meaning that a higher environmental instability is not decisive in fixing the  $N_i$  peak values. Jumping now to the  $\mathcal{N}_{sg} = 10$  and 50 cases, we retrieve the dramatic increase of  $N_i$  due to an increasing CIBU efficiency. The enhancement is locally as high as one thousand fold in the strongest case ( $\mathcal{N}_{sg} = 50$ ). There are also other noteworthy features: an increase of the  $N_i$  area coverage with  $\mathcal{N}_{sg}$  (less visible in the "Low"  
430 CAPE case) and a higher CTH which exceeds 13 km for the "Mid" and "High" CAPE cases. All these observations strongly suggest that convection is invigorated when the CIBU effect is increased.

In contrast, the simulations run with  $\mathcal{N}_{sg}=\text{RANDOM}$  with values taken in the 0.1-10 range (see Section 2.1), show a moderate effect of CIBU. Locally,  $N_i$  values reach  $1 \times 10^4 \text{ kg}^{-1}$ , which is one hundred less than  $N_i$  peak values in the  $\mathcal{N}_{sg} = 50$  cases but approximately, ten times more than in the "no CIBU" case ( $\mathcal{N}_{sg} = 0$ ). Finally the simulation results suggest that the  $\mathcal{N}_{sg}$  parameter could be constrained by satellite data because of the sensitivity of CIBU to the cloud ice coverage and the cloud top height.

## 4.2 Sensitivity to the precipitation

The 4-hour accumulated precipitation maps are presented in Fig. 17. On each row, precipitation increase from the "Low" to "High" CAPE cases. This is because the CAPE is enhanced by the addition of more and more water vapour to the atmosphere. Looking now at the sensitivity of the accumulated precipitation to  $\mathcal{N}_{sg}$ , it is not easy to draw a general conclusion on the decrease of the precipitation peak with  $\mathcal{N}_{sg}$  as for the STERAO case (see section 3.1). The reason is the highly concentrated precipitation field, which leads to a sharp gradient around the location of the peak value. However, the decrease of the precipitation with  $\mathcal{N}_{sg}$  is observed in the "Low" and "High" CAPE cases. In the "Mid" case, the precipitation peak value remains high when  $\mathcal{N}_{sg} = 50$  but the area where the precipitation is less than 10 mm shrinks continuously. The reduction of the area where the precipitation amount is greater than 10 mm when  $\mathcal{N}_{sg}$  is increased, operates in all CAPE cases (not shown).

In conclusion, the simulations illustrate the fact that the precipitation patterns are affected by the value of the  $\mathcal{N}_{sg}$  parameter. When  $\mathcal{N}_{sg}$  is increased from zero up to 50, the precipitation is reduced, either for the peak value or at least for the precipitating area. This is consistent with our previous results concerning the STERAO case. The conversion efficiency of the small ice crystals to precipitating ice particles is lower when the cloud ice concentration is high because the deposition growth of individual small crystals is limited by the amount of supersaturated water vapour available.

## 4.3 Sensitivity to the ice thickness

The last analysis is concerned with the ice thicknesses computed as the integral along the vertical of  $\rho_{dref} V_x$  where  $r_x$  refers to the mixing ratio with  $x \in i, s, g$  standing for the cloud ice, the snow-aggregates and the graupel-hail, respectively. Fig. 18 displays the total ice thickness, a sum of three terms, in mm (coloured area) with the superimposed cloud ice thickness (THIC), contoured at 1 mm. A remarkable feature is that the total ice thickness seems almost insensitive to the CIBU process for a given CAPE case as there is no great modification in the plots when moving from  $\mathcal{N}_{sg} = 0$  to  $\mathcal{N}_{sg} = 50$ . This is in contrast with the cloud ice thickness, for which the area increases with  $\mathcal{N}_{sg}$ . The rise in the maximum value of THIC was also expected for growing values of  $\mathcal{N}_{sg}$ . However, the increase of  $\text{THIC}_{\max}$  with the CAPE is much more moderate between the "Low" and "High" cases because a

higher CAPE regime with higher humidity tends to favour the horizontal spread of the cloud ice mass more.

## 5 Summary and perspectives

470 The aim of this work was to study a comprehensive parameterization of the Collisional Ice Break-Up for a bulk 2-moment microphysics scheme LIMA running in a cloud resolving mesoscale model (Meso-NH in our case). While the process is ~~strongly~~ suspected to occur in real clouds, it is not included in current bulk microphysics schemes. Because of uncertainties, the present parameterization has been kept as simple as possible. It considers only collisions between small aggregates and  
475 large dense graupel particles. The number of ice fragments that results from a single ~~shock~~collision,  $\mathcal{N}_{sg}$ , is a key parameter ~~which is only estimated from~~, which is estimated from only very few past experiments (Vardiman, 1978). A merit of this study is to ~~provide~~ suggest an upper bound to the value of  $\mathcal{N}_{sg}$  because of the sensitivity of  $\mathcal{N}_{sg}$  to the simulated precipitation. We found that taking  $\mathcal{N}_{sg} > 10$  ~~reduces significantly~~ significantly reduces the precipitation at the ground. This is ~~not~~  
480 ~~acceptable~~ problematic since most of the cloud schemes (running without the CIBU process) are tuned for quantitative precipitation forecasts. ~~Furthermore~~ Going further, we suggest ~~to consider that~~  $\mathcal{N}_{sg}$  could be considered as the realization of a random process because delicate radiating crystals undergoing fragmentation lead to a variety of crystals with a missing arm or to many irregular fragments as illustrated and discussed by Hobbs and Farber (1972). As a result, it has been shown, ~~for~~  
485 ~~instance, that running that running~~ LIMA with  $\mathcal{N}_{sg} > 10$  ~~in the STERAO deep convection test case,~~ dramatically for the STERAO and WK deep convection cases, alters the precipitation at the ground because the conversion of cloud ice crystals into precipitating ice is slowed down. ~~Simultaneously,~~ ~~a major expected effect of CIBU is clearly to increase~~ In any case, the increase of the number concentration of the small ice crystals due to the application of CIBU is clearly significant (up to one  
490 thousand fold in the WK simulations with  $\mathcal{N}_{sg} = 50$ ).

The microphysics perturbation due to the activation of CIBU has been studied in detail for the STERAO case by looking at the profiles of the mixing ratios, ice concentrations and corresponding budget terms. In particular, the CIBU effect on the pristine ice and aggregate mixing ratios is compensated by an enhancement of the capture of the small crystals by the aggregates. The sensitivity of  
495 the ice concentration to  $\mathcal{N}_{sg}$  is demonstrated with a mean ~~multiplication~~ multiplication factor as high as 25 for  $\mathcal{N}_{sg} = 10$ . The last study on the sensitivity of the simulations to the initial IFN concentration showed that CIBU was mostly efficient for current IFN concentrations of  $\sim 1 \text{ dm}^{-3}$ . Furthermore, the CIBU process was still active for very low IFN concentrations, down to  $0.001 \text{ dm}^{-3}$ , which were sufficient to initiate the ice phase.

500 The effects of CIBU have been confirmed by the additional WK simulations. The enhancement of the cloud ice concentration is very high when  $\mathcal{N}_{sg} > 10$  and a loss of surface precipitation (peak

value and reduction of the precipitating areas) is found. Higher ice concentrations lead to a larger coverage of ice clouds and higher cloud tops for the most vigorous convective cells. In contrast, the total ice thickness is almost insensitive to CIBU. An increase of cloud ice mass with  $\mathcal{N}_{sg}$  is balanced by a slight decrease of the precipitating ice (aggregates and graupels).

The proposed parameterization is very easy to implement and to evaluate. It would be useful to evaluate it in other microphysics schemes where the conversion of the cloud ice and the growth of precipitating ice is represented (aggregates and rimed particles) are treated differently. The tuning basic adjustment of the scheme can be revised as soon as laboratory experiments are available for fixing more precisely more precise fixing of the sizes and the shapes of the crystals that break following collisions, to examine any possible thermal effect and to estimate the variety of fragment numbers more accurately. However, as microphysics schemes are now used to produce quantitative precipitation forecasts, it is also imperative to check that the production of rain is not too much altered by an overestimated CIBU effect. Another way to determine the acceptable range of values for  $\mathcal{N}_{sg}$  is to work with satellite data, as the WK experiments demonstrated an enhancement of the cloud top ice cover (and possibly the cloud top height) with  $\mathcal{N}_{sg}$ .

With new imagers, counters and improvements in data analysis (Ladino et al., 2017), more and more evidence is being presented that ice multiplication production is a dominant is an essential process in natural deep convective clouds. However, the explanation of anomalously high ice crystal concentrations is still difficult to link to a precise process (Rangno and Hobbs, 2001; Field et al., 2017). So the next step in the LIMA scheme is to introduce the shattering of the raindrops during freezing as proposed by Lawson et al. (2015) and to compare with CIBU, because the basic in order to complete the LIMA scheme, since the different ingredients, raindrops and small ice crystals, leading to a different ice multiplication process are not the same. Then, the final task is to check that microphysics schemes with all offer another pathway for ice multiplication. A task is then to study whether all the known sources of small ice crystals, nucleation and secondary ice production, are able to cooperate and to reproduce observed ice concentrations which can reach in microphysics schemes to reproduce the very high values (units of  $\text{cm}^{-3}$ ) in deep convective clouds but without convincing explanation yet of ice concentrations sometimes observed. Quantitative cloud data gathered in the tropics during HAIC/HIWC (High Altitude Ice Crystals/ High Ice water Content) field project (Leroy et al., 2015; Ladino et al., 2017) could be a starting point to evaluate the capability of high resolution cloud simulations with high ice contents to reproduce events where high cloud ice contents were recorded.

## 6 Code availability

The Meso-NH code is publicly available at <http://mesonh.aero.obs-mip.fr/mesonh51>. Here the model development and the simulations were made carried with version "MASDEV5-1 BUG2". The modi-

fications [brought made](#) to the LIMA scheme (v1.0) are available upon request from Jean-Pierre Pinty and [next](#) in the Supplement related to this article [and](#), available at <http://doi.org/10.5281/zenodo.1078527>.

## Appendix A: Moments of the gamma and incomplete gamma functions

540 The  $p^{th}$  moment of the generalized gamma function (see definition in the text) is

$$M(p) = \int_0^{\infty} D^p n(D) dD = \frac{\Gamma(\nu + p/\alpha)}{\Gamma(\nu)} \frac{1}{\lambda^p} \quad (A1)$$

where the gamma function is defined as:

$$\Gamma(x) = \int_0^{\infty} t^{x-1} e^{-t} dt. \quad (A2)$$

The  $p^{th}$  moment of the incomplete gamma function is written

$$545 \quad M^{INC}(p; X) = \int_0^X D^p n(D) dD. \quad (A3)$$

The algorithm of the "GAMMA\_INC( $p; X$ )" function (Press et al., 1992) is useful to tabulate  $M^{INC}(p; X) \times \Gamma(p)$  in addition to the "GAMMA" function algorithm of Press et al. (1992). A change of variable is necessary to take the generalized form of the gamma size distributions into account. As a result,  $M^{INC}(p; X)$  is written:

$$550 \quad M^{INC}(p; X) = M(p) \times \text{GAMMA\_INC}(\nu + p/\alpha; (\lambda X)^\alpha) \quad (A4)$$

with  $M(p)$  given by Eq. A1.

*Acknowledgements.* J.-P. Pinty wishes to thank V. Phillips for discussions about his original work on the topic. This work was done during the PhD of T. Hoarau who is financially supported by Reunion Island Regional Council and the European Union Council. T. Hoarau thanks [the](#) University of La Réunion for supporting a  
555 short stay at [the](#) Laboratoire d'Aérodologie. Mrs Susan Becker corrected the English of the manuscript. Preliminary computations were performed on the 36 node home-made cluster of Lab. Aérodologie. J.-P. Pinty acknowledges CALMIP (CALcul MIDI-Pyrénées) of the University of Toulouse for access to the "[Eoseos](#)" supercomputer where useful additional simulations were performed. T. Hoarau and C. Barthe acknowledged the GENCI resources for access to the "Occigen" supercomputer. [This work was supported by the French national programme LEFE/INSU through the LIMA-TROPIC project.](#)  
560 [The authors thank the reviewers for their pertinent comments which helped to ~~improved a lot~~ greatly improve](#) the first version of the manuscript.

## References

- Colella, P. and Woodward, P.: The piecewise parabolic method (PPM) for gas-dynamical simulations, *J. Comput. Phys.*, 54, 174–201, 1984.
- 565 Dye, J. E., Ridley, B. A., Skamarock, W., Barth, M., Venticinque, M., Defer, E., Blanchet, P., Théry, C., Laroche, P., Baumann, K., Hubler, G., Parrish, D. D., Ryerson, T., Trainer, M., Frost, G., Holloway, J. S., Matejka, T., Bartels, D., Fehsenfeld, F. C., Tuck, A., Rutledge, S. A., Lang, T., Stith, J., and Zerr, R.: An overview of the Stratospheric-Tropospheric Experiment: Radiation, Aerosols, and Ozone (STERAO)-Deep Convection experiment with results for the July 10, 1996 storm, *J. Geophys. Res.*, 105, 10,023–10,045, doi:10.1029/1999JD901116, 2000.
- 570 Field, P. R.: Bimodal ice spectra in frontal clouds, *Quart. J. Roy. Meteor. Soc.*, 126, 379–392, doi:10.1002/qj.49712656302, 2000.
- Field, P. R., Lawson, R. P., Brown, P. R. A., Lloyd, G., Westbrook, C., Moisseev, D., Miltenberger, A., Nenes, A., Blyth, A., Choulaton, T., Connolly, P., Buehl, J., Crosier, J., Cui, Z., Dearden, C., DeMott, P., Flossmann, A., Heymsfield, A., Huang, Y., Kalesse, H., Kanji, Z. A., Korolev, A., Kirchgaessner, A., Lasher-Trapp, S., Leisner, T., McFarquhar, G., Phillips, V., Stith, J., and Sullivan, S.: Secondary ice production: current state of the science and recommendations for the future, *Meteor. Monogr.*, 58, 7.1–7.20, doi:10.1029/AMSMONOGRAPHS-D-16-0014.1, 2017.
- Foote, G. B. and du Toit, P. S.: Terminal velocity of raindrops, *J. Appl. Meteor.*, 8, 249–253, 1969.
- 580 Griggs, D. G. and Choulaton, T. W.: A laboratory study of secondary ice article production by the fragmentation of rime and vapour-grown ice crystals, *Quart. J. Roy. Meteor. Soc.*, 112, 149–163, doi:10.1002/qj.49711247109, 1986.
- Hallett, J. and Mossop, S. C.: Production of secondary ice particles during the riming process, *Nature*, 249, 26–28, doi:10.1038/249026a0, 1974.
- 585 Harrington, J. Y., Meyers, M. P., Walko, R. L., and Cotton, W. R.: Parameterization of Ice Crystal Conversion Processes Due to Vapor Deposition for Mesoscale Models Using Double-Moment Basis Functions. Part I: Basic Formulation and Parcel Model Results, *J. Atmos. Sci.*, 52, 4344–4366, doi:10.1175/1520-0469(1995)052<4344:POICCP>2.0.CO;2, 1995.
- Hobbs, P. V. and Farber, R. J.: Fragmentation of ice particles in clouds, *J. Rech. Atmos.*, 6, 245–258, 1972.
- 590 Hobbs, P. V. and Rangno, A. L.: Ice particle concentrations in clouds, *J. Atmos. Sci.*, 42, 2523–2549, 1985.
- Ladino, L. A., Korolev, A., Heckman, I., Wolde, M., Fridlind, A. M., and Ackerman, A. S.: On the role of ice-nucleating aerosol in the formation of ice particles in tropical mesoscale convective systems, *Geophys. Res. Lett.*, 44, doi:10.1002/2016GL072455, 2017.
- Lafore, J. P., Stein, J., Asencio, N., Bougeault, P., Ducrocq, V., Duron, J., Fischer, C., Héreil, P., Mascart, P., Masson, V., Pinty, J.-P., Redelsperger, J.-L., Richard, E., and Vila-Guerau de Arellano, J.: The Meso-NH atmospheric simulation system. Part I: adiabatic formulation and control simulations, *Annales Geophysicae*, 16, 90–109, doi:10.1007/s00585-997-0090-6, 1998.
- Lawson, R. P., Woods, S., and Morrison, H.: The microphysics of ice and precipitation development in tropical cumulus clouds, *J. Atmos. Sci.*, 72, 2429–2445, doi:10.1175/JAS-D-14-0274.1, 2015.
- 600 Leroy, D., Fontaine, E., Schwarzenboeck, A., Strapp, J. W., Lilie, L., Delanoe, J., Protat, A., Dezitter, F., and Grandin, A.: HAIC/HIWC Field Campaign - Specific findings on PSD microphysics in high IWC regions

- from in situ measurements: median mass diameters, particle size distribution characteristics and ice crystal shapes, SAE Technical Paper, doi:10.4271/2015-01-2087, 2015.
- Phillips, V. T., Yano, J.-I., and Khain, A.: Ice multiplication by break-up in ice-ice collisions. Part I: Theoretical  
605 formulation, *J. Atmos. Sci.*, 74, 1705–1719, doi:10.1175/JAS-D-16-0224.1, 2017.
- Press, W. H., Teukolsky, S. A., Vetterling, W. T., and Flannery, B. P.: *Numerical Recipes in FORTRAN: The Art of Scientific Computing*, Cambridge University Press, New-York, 1992.
- Rangno, A. L. and Hobbs, P. V.: Ice particles in stratiform clouds in the Arctic and possible mechanisms for the production of high ice concentrations, *J. Geophys. Res.*, 106, 15 065–15 075, 2001.
- 610 Skamarock, W. C., Powers, J. G., Barth, M., Dye, J. E., Matejka, T., Bartels, D., Baumann, K., Stith, J., Parrish, D. D., and Hübner, G.: Numerical simulations of the July 10 Stratospheric-Tropospheric Experiment: Radiation, Aerosol, and Ozone/Deep Convection Experiment convective system: Kinematics and transport, *J. Geophys. Res.*, 105, 19,973–19,990, 2000.
- Sullivan, S. C., Hoose, C., and Nenes, A.: Investigating the contribution of secondary ice production to in-cloud  
615 ice crystal numbers, *J. Geophys. Res.*, 122, doi:10.1002/2017JD026 546, 2017.
- Sullivan, S. C., Hoose, C., Kiselev, A., Leisner, T., and Nenes, A.: Initiation of secondary ice production in clouds, *Atmos. Chem. Phys.*, 18, doi:10.5194/acp-18-1593-2018, 2018.
- Takahashi, T., Nagao, Y., and Kushiyama, Y.: Possible high ice particle production during graupel-graupel collisions, *J. Atmos. Sci.*, 52, 4523–4527, 1995.
- 620 Vardiman, L.: The generation of secondary ice particles in clouds by crystal–crystal collision, *Journal of the Atmospheric Sciences*, 35, 2168–2180, doi:1520-0469(1978)035<2168:TGOSIP>2.0.CO;2, 1978.
- Vié, B., Pinty, J.-P., Berthet, S., and Leriche, M.: LIMA (v1.0): A quasi two-moment microphysical scheme driven by a multimodal population of cloud condensation and ice freezing nuclei, *Geoscientific Model Development*, 9, 567–586, doi:10.5194/gmd-9-567-2016, 2016.
- 625 Weisman, M. L. and Klemp, J. B.: The dependence of numerically simulated convective storms on vertical wind shear and buoyancy, *Mon. Wea. Rev.*, 110, 504–520, 1982.
- Weisman, M. L. and Klemp, J. B.: The structure and classification of numerically simulated convective storms in directionally varying wind shear, *Mon. Wea. Rev.*, 112, 2479–2498, 1984.
- Yano, J.-I. and Phillips, V. T.: Ice–Ice Collisions: An Ice Multiplication Process in Atmospheric Clouds, *J.*  
630 *Atmos. Sci.*, 68, 322–333, doi:10.1175/2010JAS3607.1, 2011.
- Yano, J.-I. and Phillips, V. T.: Explosive Ice Multiplication Induced by multiplicative-Noise fluctuation of Mechanical Break-up in Ice-Ice Collisions, *J. Atmos. Sci.*, 73, 4685–4697, doi:10.1175/JAS-D-16-0051.1, 2016.
- Yano, J.-I., Phillips, V. T., and Kanawade, V.: Explosive ice multiplication by mechanical break-up in ice–ice collisions: a dynamical system-based study, *Quart. J. Roy. Meteor. Soc.*, 142, 867–879, doi:10.1002/qj.2687,  
635 2016.

CCN	Aitken mode	Accumulation mode	Coarse mode
$N$ ( $\text{cm}^{-3}$ )	300	140	50
$d_X$ ( $\mu\text{m}$ )	0.23	0.8	2.0
$\sigma_X$	2.0	1.5	1.6

IFN	Dust mode	BC+Organics mode
$N$ ( $\text{dm}^{-3}$ )	10	10
$d_X$ ( $\mu\text{m}$ )	0.8	0.2
$\sigma_X$	2.0	1.6

**Table 1.** Background CCN and IFN configuration for the STERAO idealized case simulations.

$\mathcal{N}_{sg}$ (no unit)	0.0	0.1	1.0	2.0	5.0	10.0	20.0	50
$N_i$ ( $\#kg^{-1}$ )	790	940	1,160	1,860	8,000	25,670	62,010	112,740
CIBU <sub>ef</sub> (%)	0	19	47	135	913	3149	7749	14171

**Table 2.** After 3 hours of simulation, maximum value of the cloud ice number concentration  $N_{i_{max}}$  as a function of the number of fragments produced per snow/aggregate-graupel collision  $\mathcal{N}_{sg}$ . The last row is the CIBU enhancement factor CIBU<sub>ef</sub> in percent (see text).

Process Acronym	Description
ACC	Raindrop accretion on snow to produce graupel
AGGS	Snow growth by capture of cloud ice
BERFI	Growth of cloud ice by Bergeron-Findeisen process
CEDS	Deposition/sublimation of water vapour on cloud ice
CFRZ	Raindrop Freezing by contact with cloud ice
CIBU	Snow break-up by collision with graupel
CMEL	Conversion Melting of snow into graupel
CNVI	Decreasing snow converted back to cloud ice
CNVS	Growing cloud ice converted into snow
DEPG	Water vapour deposition on graupel
DEPS	Water vapour deposition on snow
DRYG	Graupel dry growth (water can freeze fully)
HINC	Heterogeneous nucleation by immersion
HIND	Heterogeneous nucleation by deposition
HONC	Homogeneous freezing of the cloud droplets
HONH	Haze homogeneous freezing
HMG	Droplet riming and Hallett-Mossop process on graupel
HMS	Droplet riming and Hallett-Mossop process on snow
<del>HMS</del> <del>Water vapour deposition on snow</del> IMLT	Melting of cloud ice
RIM	Riming of cloud droplets on snow to produce graupel
SEDI	Sedimentation of cloud ice, snow or graupel
WETG	Graupel wet growth (water is partially frozen)

**Table 3.** Nomenclature of the microphysics processes of the budget profiles.

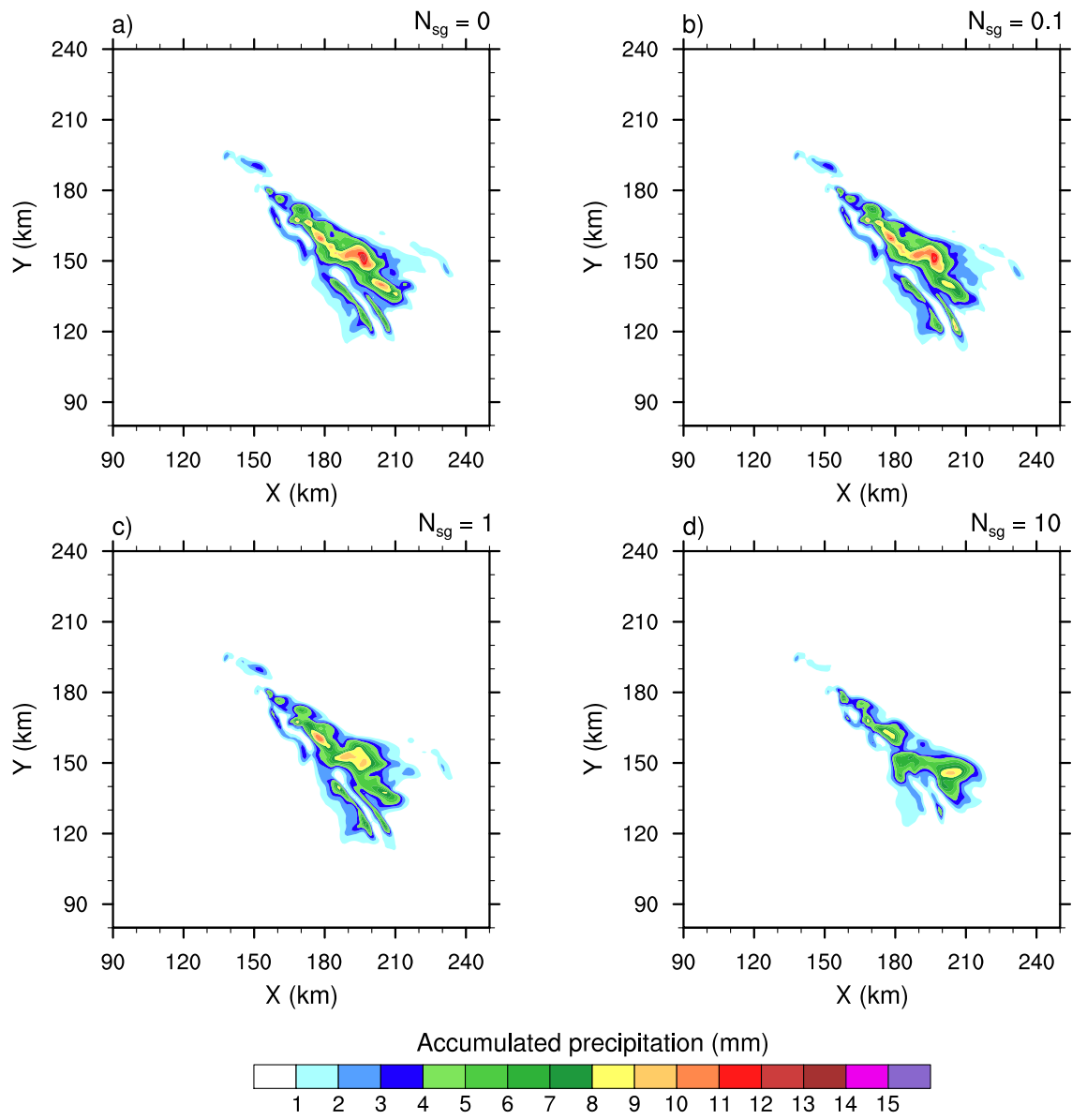


**Figure 1.** 4-h accumulated precipitation of the STERAO simulations where a) to d) refers to cases with  $N_{sg}=0.0, 0.1, 1.0$  and  $10.0$  ice fragments per collision, respectively. The plots are for a fraction of the computational domain.

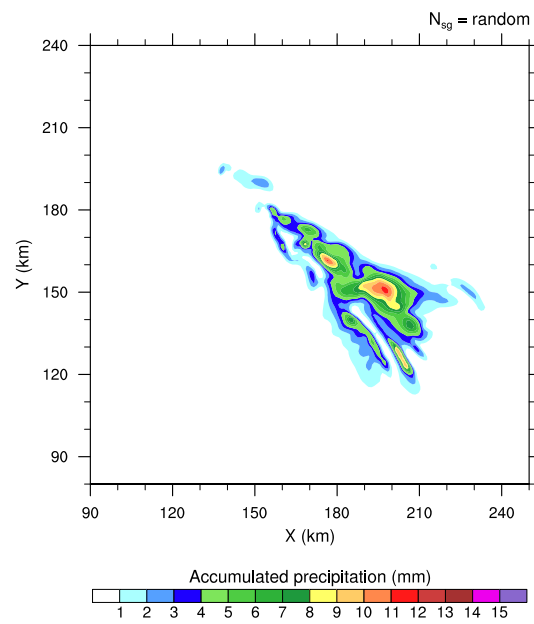


**Figure 2.** Same as Fig. 1, but for the "RANDOM" simulation.

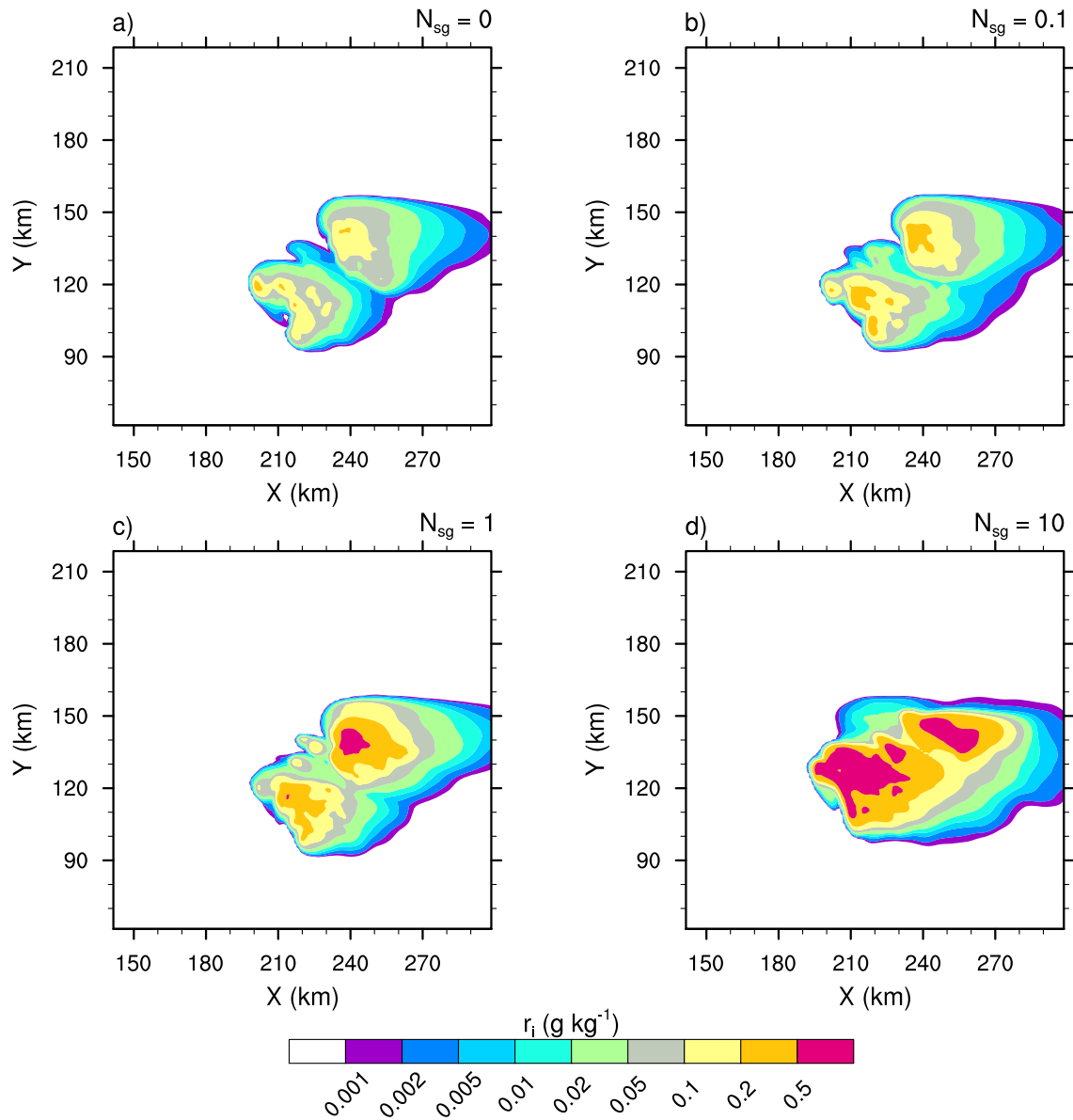


**Figure 3.** Mixing ratios of the cloud ice ( $r_i$  in log scale) of the STERAO simulations at 12 km height, where a) to d) refer to cases with  $N_{sg}=0.0, 0.1, 1.0$  and  $10.0$  ice fragments per collision, respectively. The plots are for a fraction of the computational domain.

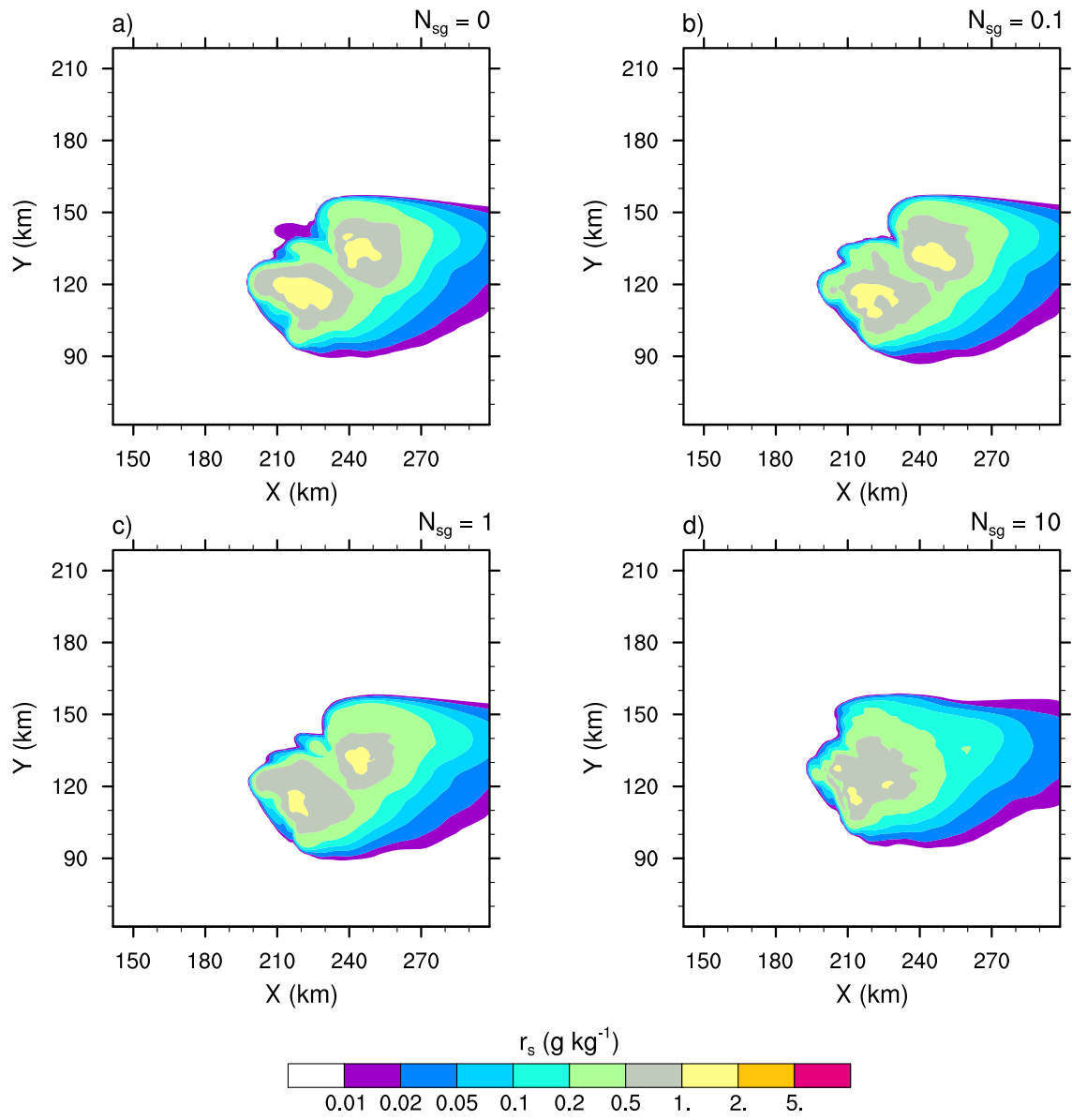


**Figure 4.** Same as Fig. 3 but for the mixing ratios of snow-aggregates ( $r_s$ ).

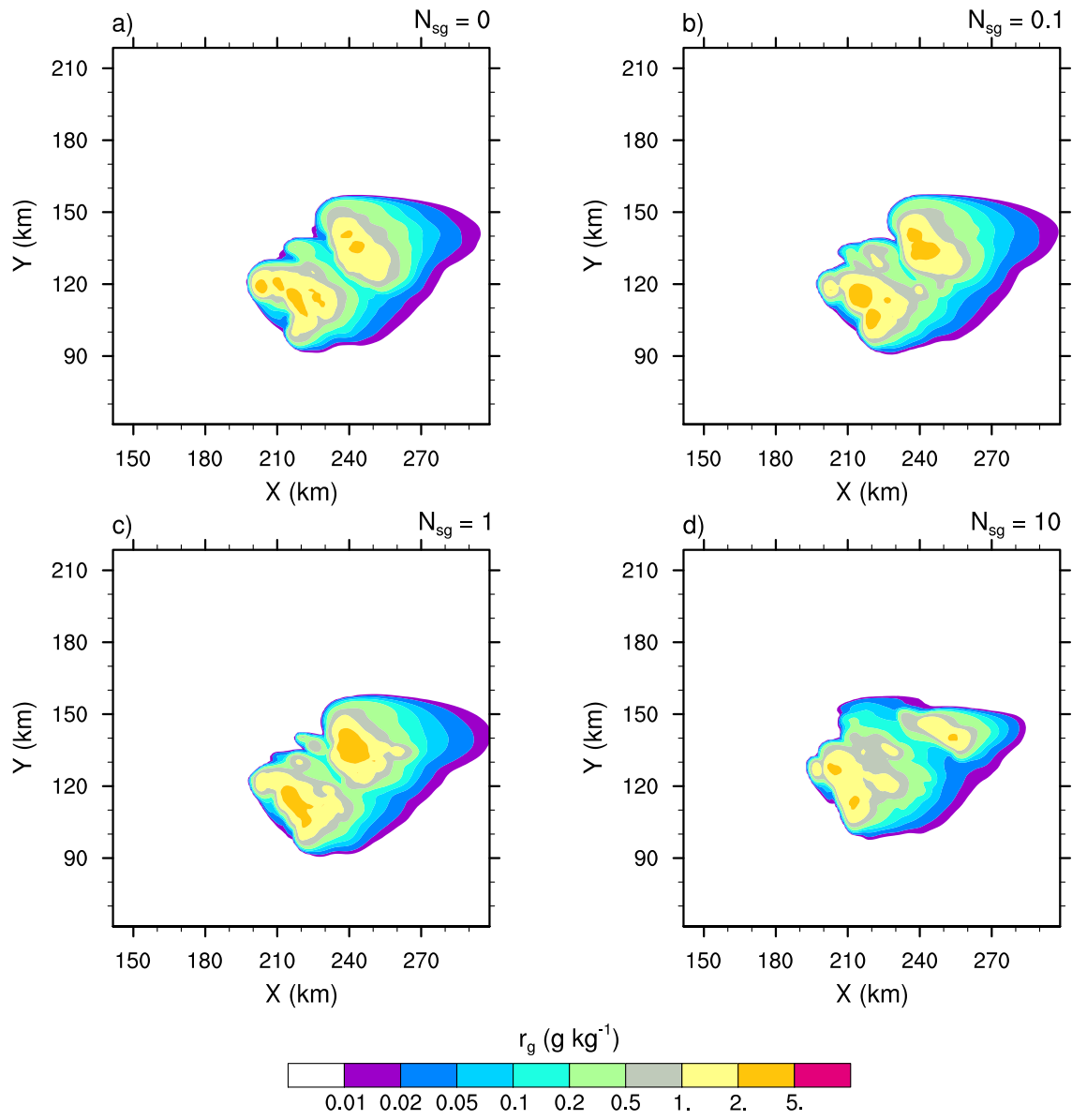


**Figure 5.** Same as Fig. 3 but for the mixing ratios of graupel ( $r_g$ ).

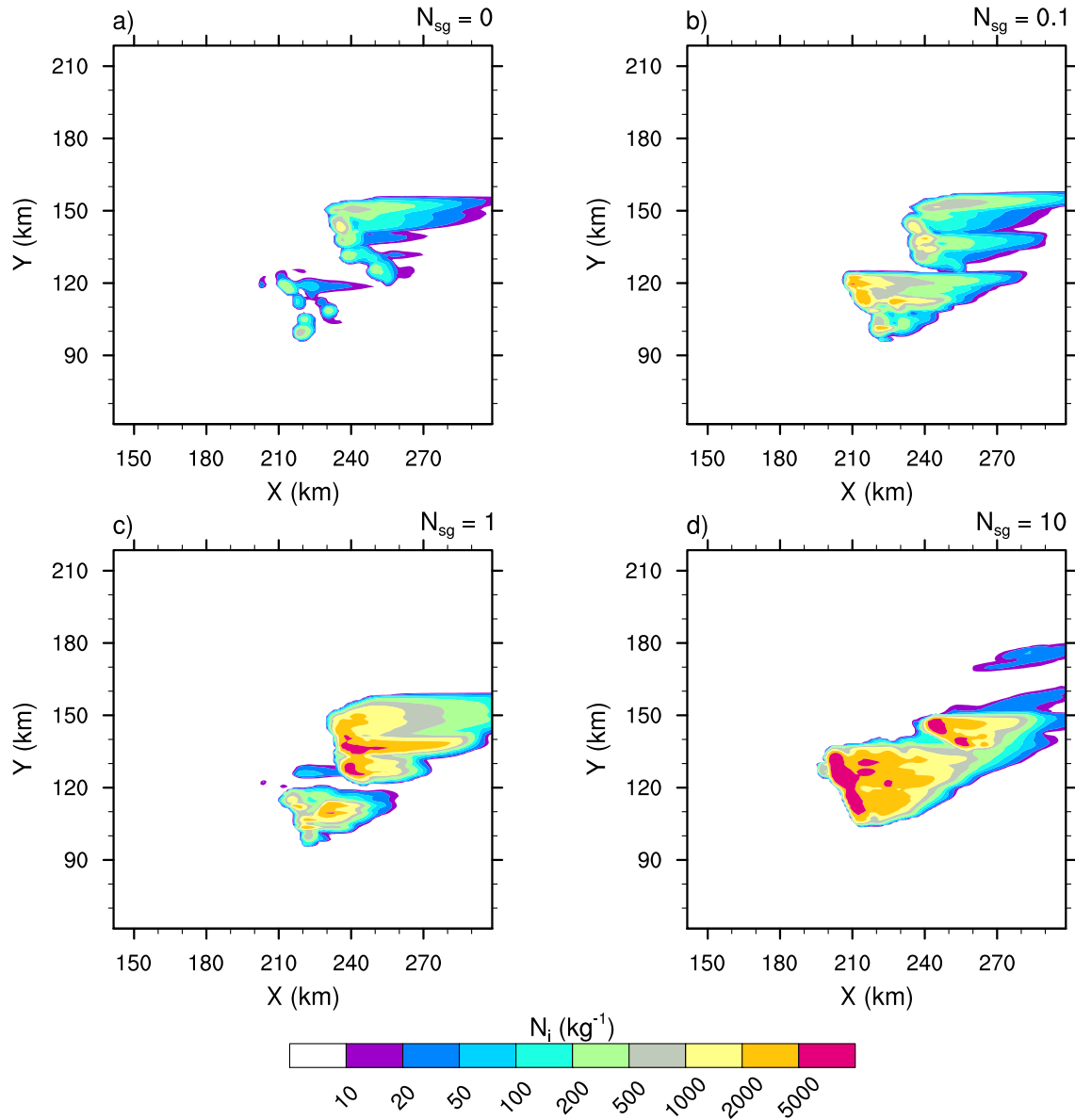


**Figure 6.** Number concentration of the cloud ice ( $N_i$  in log scale) of the STERAO simulations at 15 km height, where a) to d) refer to cases with  $\mathcal{N}_{sg}=0.0, 0.1, 1.0$  and  $10.0$  ice fragments per collision, respectively. The plots are for a fraction of the computational domain.

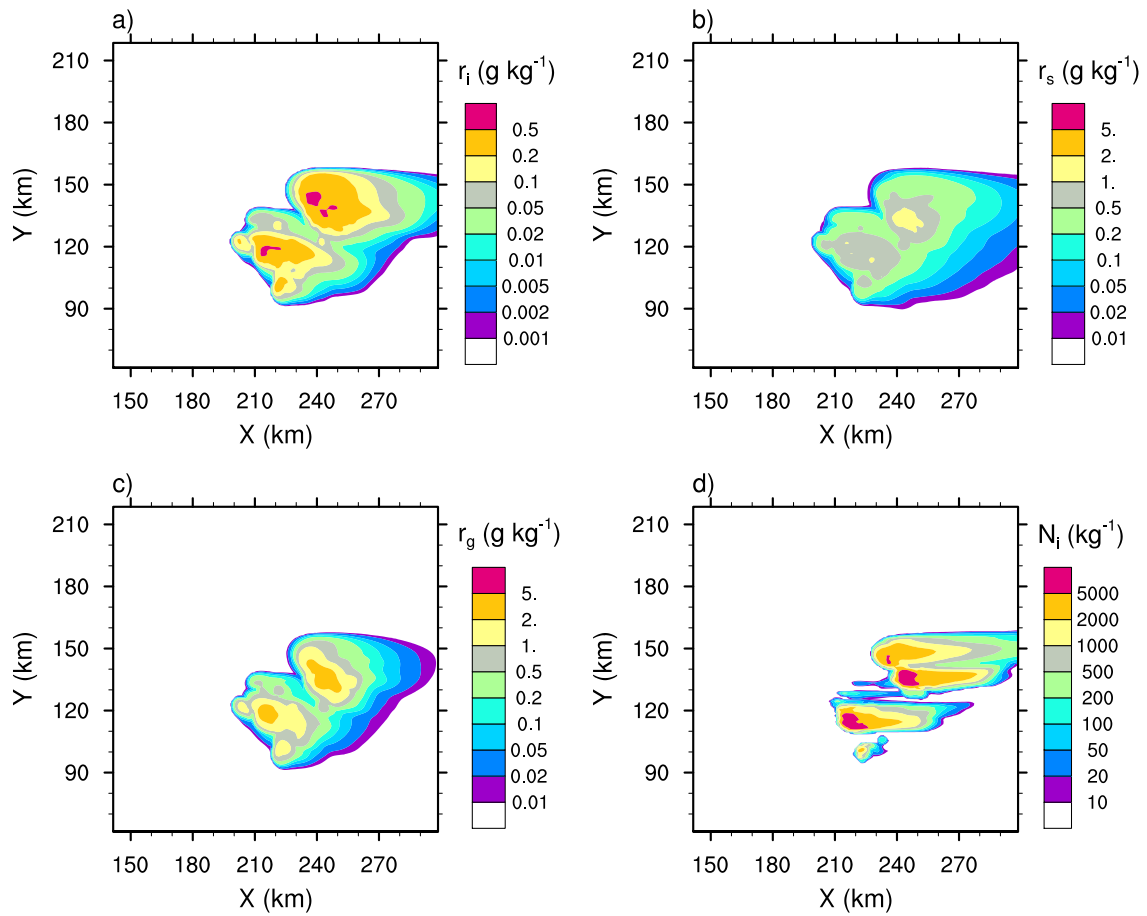


**Figure 7.** "RANDOM" case of the STERAO simulations showing the mixing ratios of a) the cloud ice ( $r_i$ ), b) the snow-aggregates ( $r_s$ ), and c) the graupel ( $r_g$ ) at 12 km height. Plot d) refers to the number concentration of the cloud ice crystals ( $N_i$ ) at 15 km height. The plots are for a fraction of the computational domain.

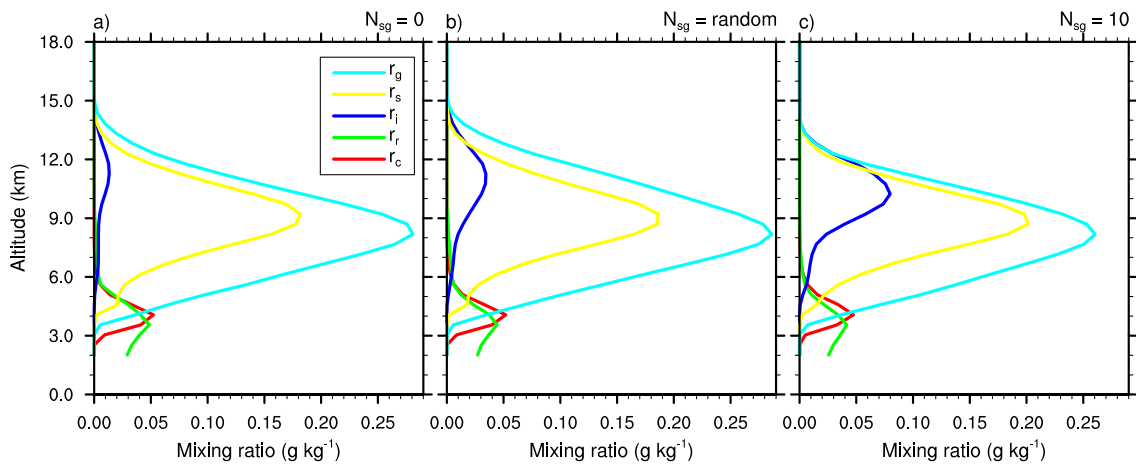


**Figure 8.** Mean profiles of condensate mixing ratios  $r_c, r_r, r_i, r_s$  and  $r_g$  ; in  $\text{g kg}^{-1}$ ) of the STERAO simulations corresponding to a) the  $\mathcal{N}_{sg}=0.0$  case, b) the "RANDOM" case and c) the case with  $\mathcal{N}_{sg} = 10.0$ .

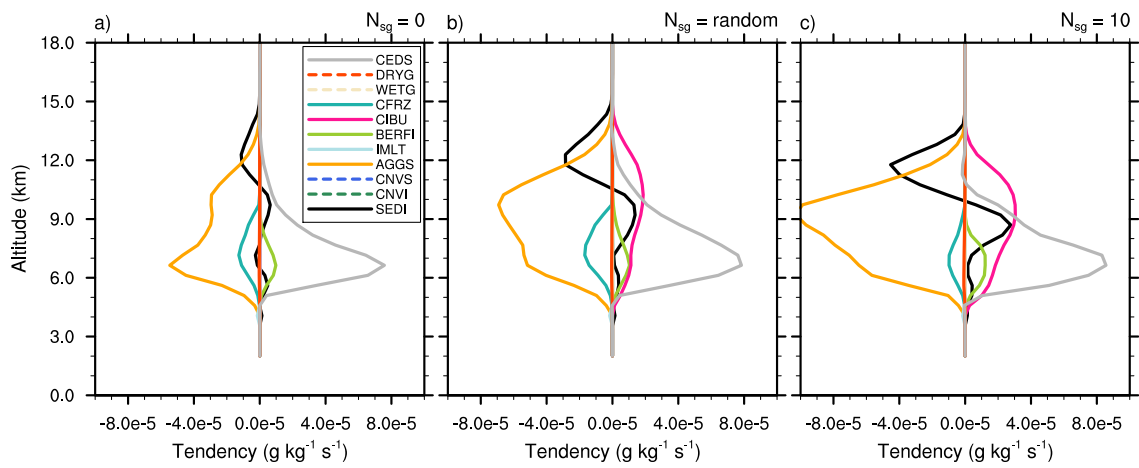


**Figure 9.** Mean microphysics profiles of cloud ice mixing ratio tendencies of the STERAO simulations corresponding to a) the  $\mathcal{N}_{sg} = 0.0$  (no CIBU) case, b) the "RANDOM" case and c) the case with  $\mathcal{N}_{sg} = 10.0$ . The dashed lines are associated with processes having no significant impact on these budgets.

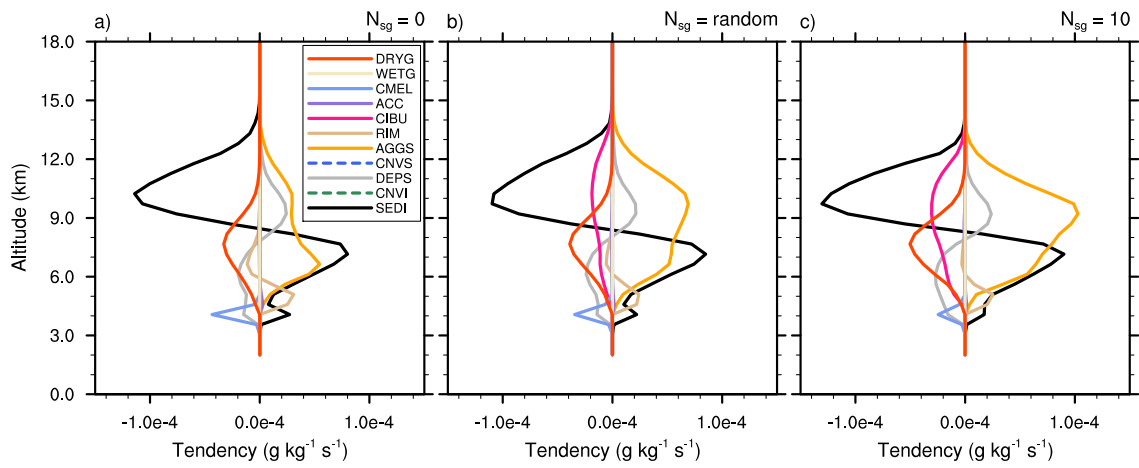


**Figure 10.** Same as Fig. 9 but for snow-aggregates.

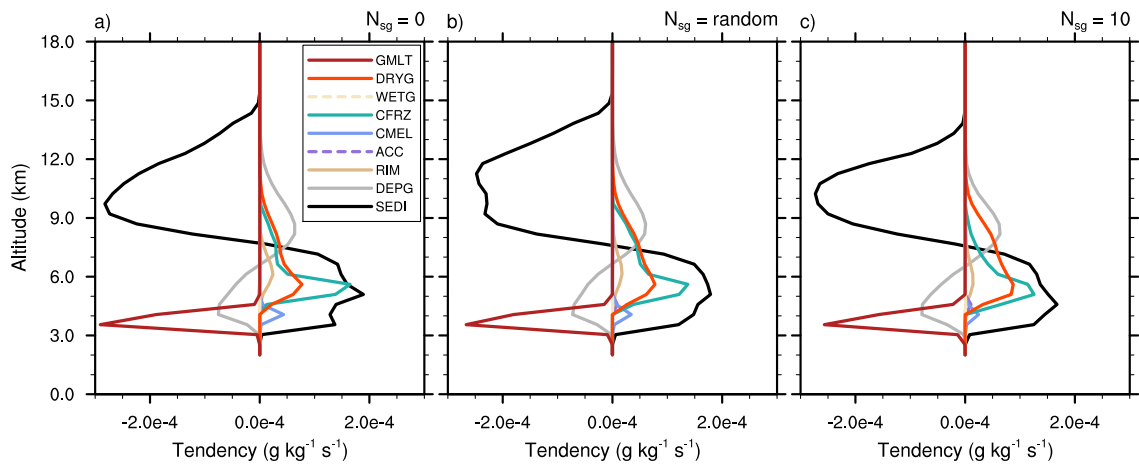


**Figure 11.** Same as Fig. 9 but for graupel.

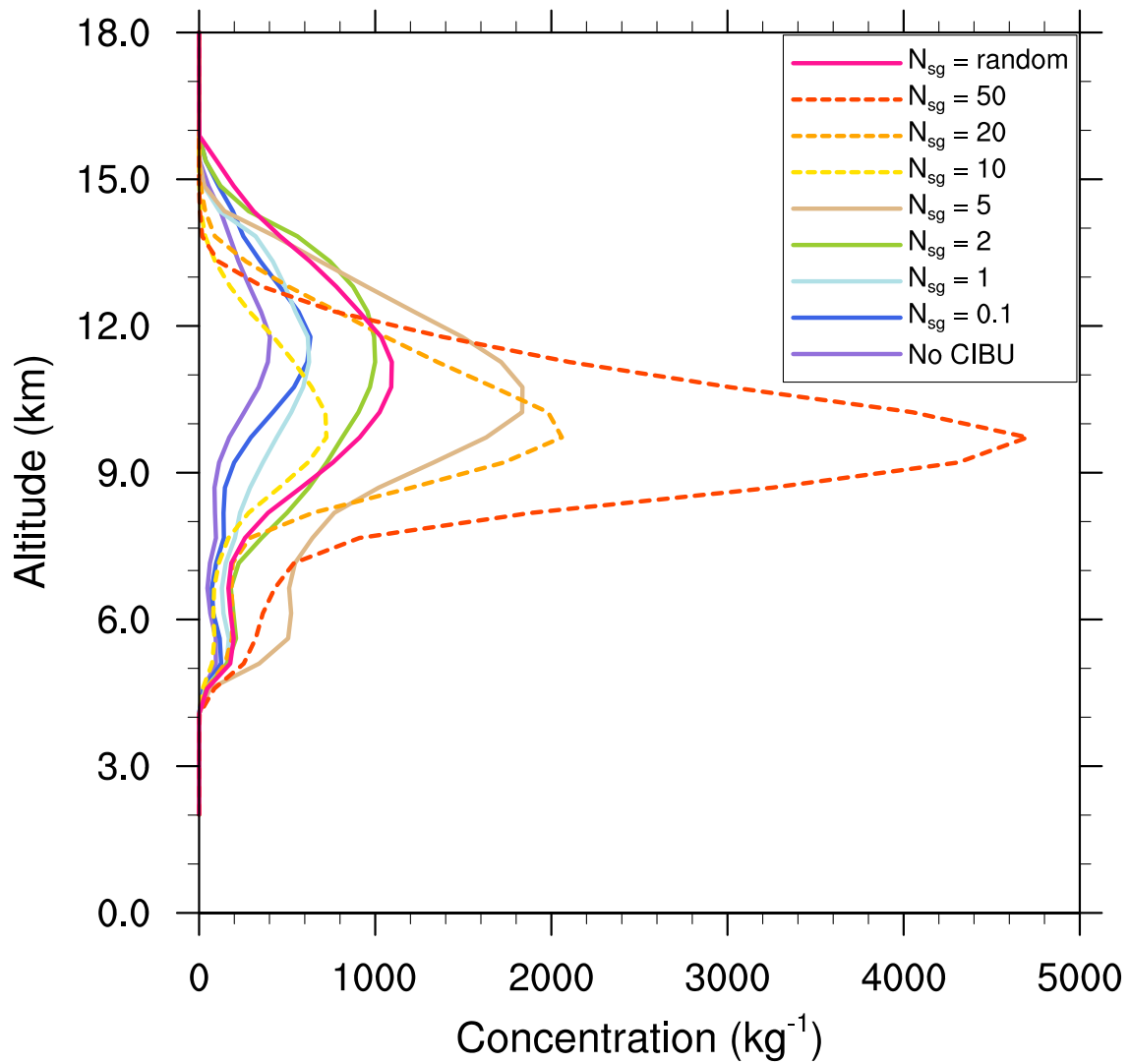


**Figure 12.** Mean profiles of the cloud ice crystal concentrations  $N_i$  ( $\text{g kg}^{-1}$ ) of the STERAO simulations corresponding to different values of  $N_{sg}$  (see the legend for details). The profiles drawn with a dashed line have been divided by 10 to fit into the plot.

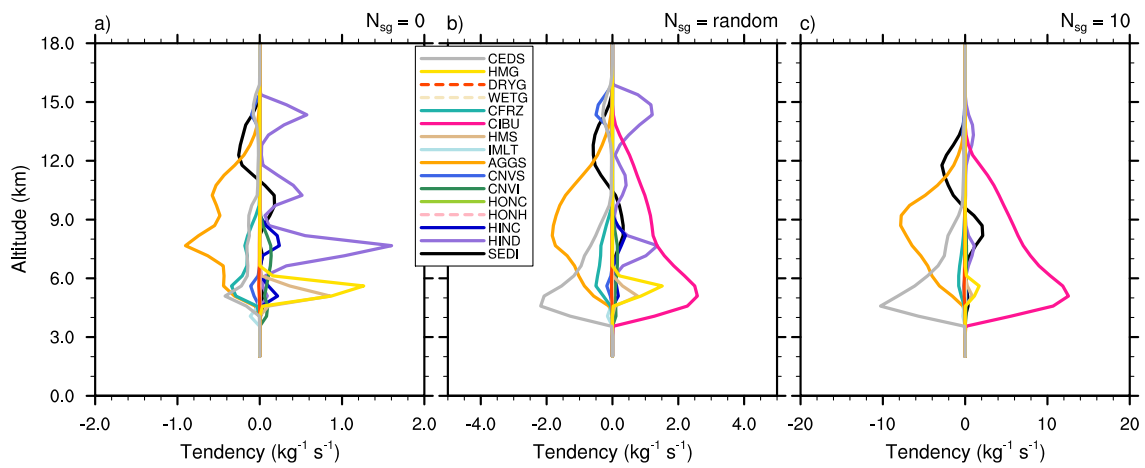


**Figure 13.** Mean microphysics profiles of the cloud ice crystal concentration tendencies of the STERAO simulations corresponding to a) the  $\mathcal{N}_{sg} = 0.0$  (no CIBU) case, b) the "RANDOM" case and c) the case with  $\mathcal{N}_{sg} = 10.0$  (Note that the horizontal scale increases from a) to c)). The dashed lines of the list box are associated with processes having no significant impact on these budgets.

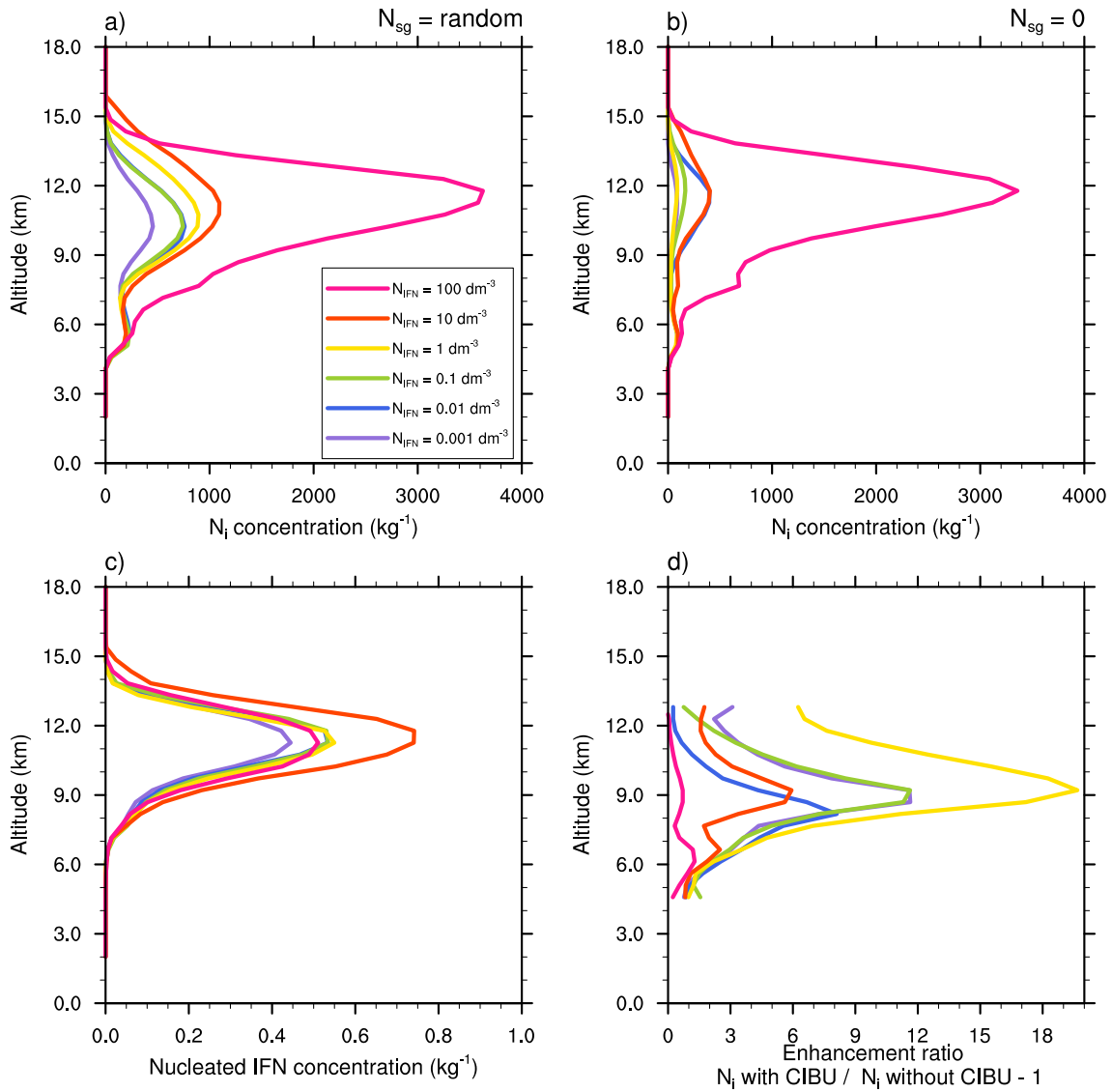


**Figure 14.** Mean profiles of cloud ice crystal concentration for 6 decades of initial IFN concentrations from 100  $dm^{-3}$  to 0.001  $dm^{-3}$  of the STERAO simulations corresponding to a) the CIBU simulation and "RANDOM" case and b) the non-CIBU simulation. The mean profiles of the nucleated IFN concentrations are plotted in c) after rescaling to fit the [0.0-1.0] range. The rough estimate of CIBU enhancement factor of  $N_i$  is plotted in d) as a function of the initial IFN concentrations.

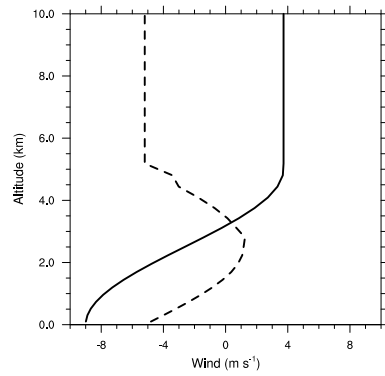


**Figure 15.** Vertical profile of the horizontal wind components of the WK84 simulations. The solid line with a constant shear ( $2.5 \times 10^{-2} \text{ s}^{-1}$ ) refers to  $U$ , the  $x$ -component of the wind and the dashed line with a jet-like structure, refers to  $V$ , the  $y$ -component of the wind.  $U$  and  $V$  are constant above 5 km height.

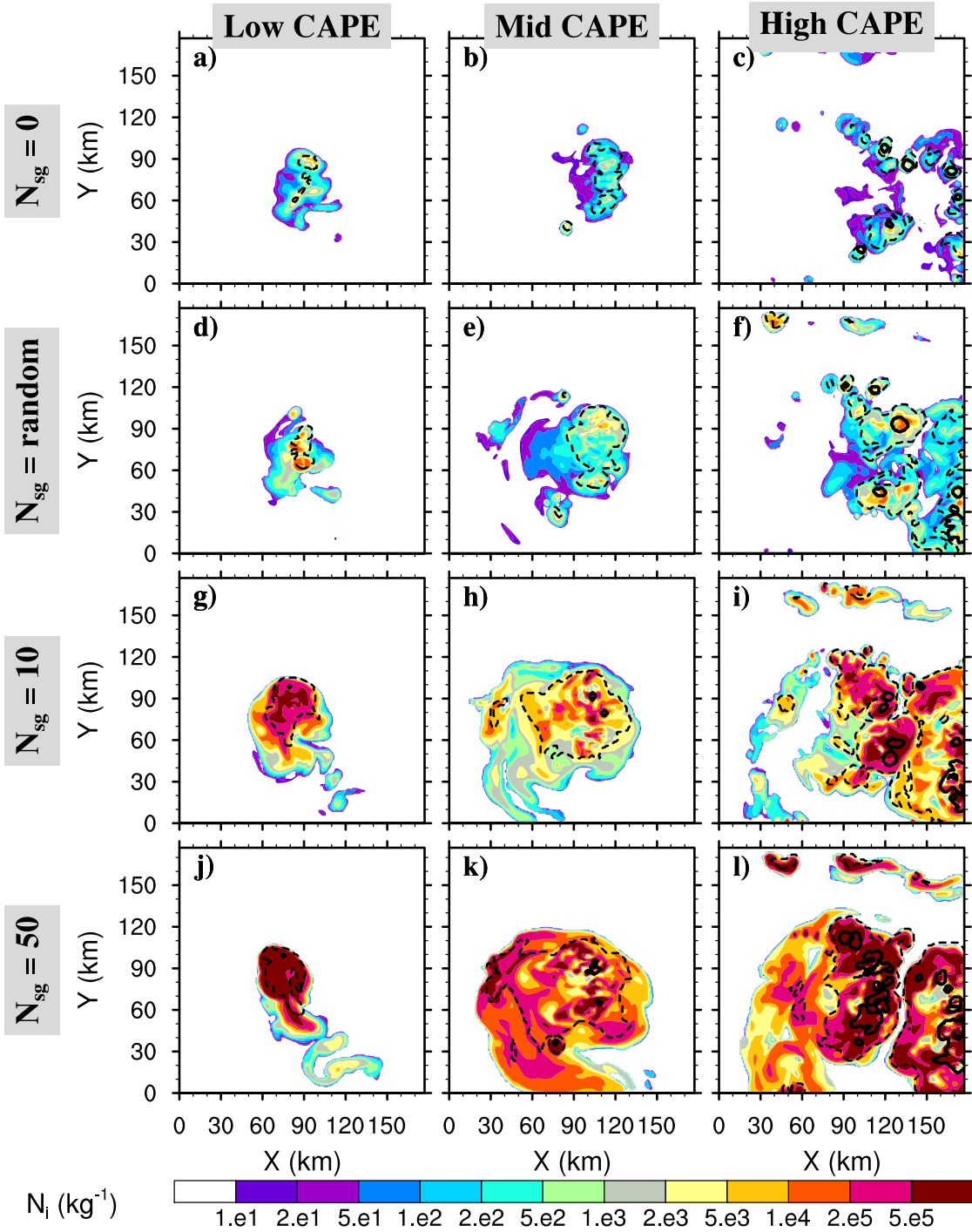


Figure 16. Small ice concentration  $N_i$  average between 9.5 and 10.5 km height after 4 hours of the WK84 simulations, where a) to c) refer to no CIBU cases ( $N_{sg}=0.0$ ), d) to f) to cases with random CIBU ( $0.1 < N_{sg} < 10$ ) and g) to i) to cases with a high CIBU effect ( $N_{sg}=10.0$ ), and j) to l) to cases with an intense CIBU effect ( $N_{sg}=50.0$ ). The isocontours are the cloud top heights with dotted lines for 11 km and solid lines for 13 km.

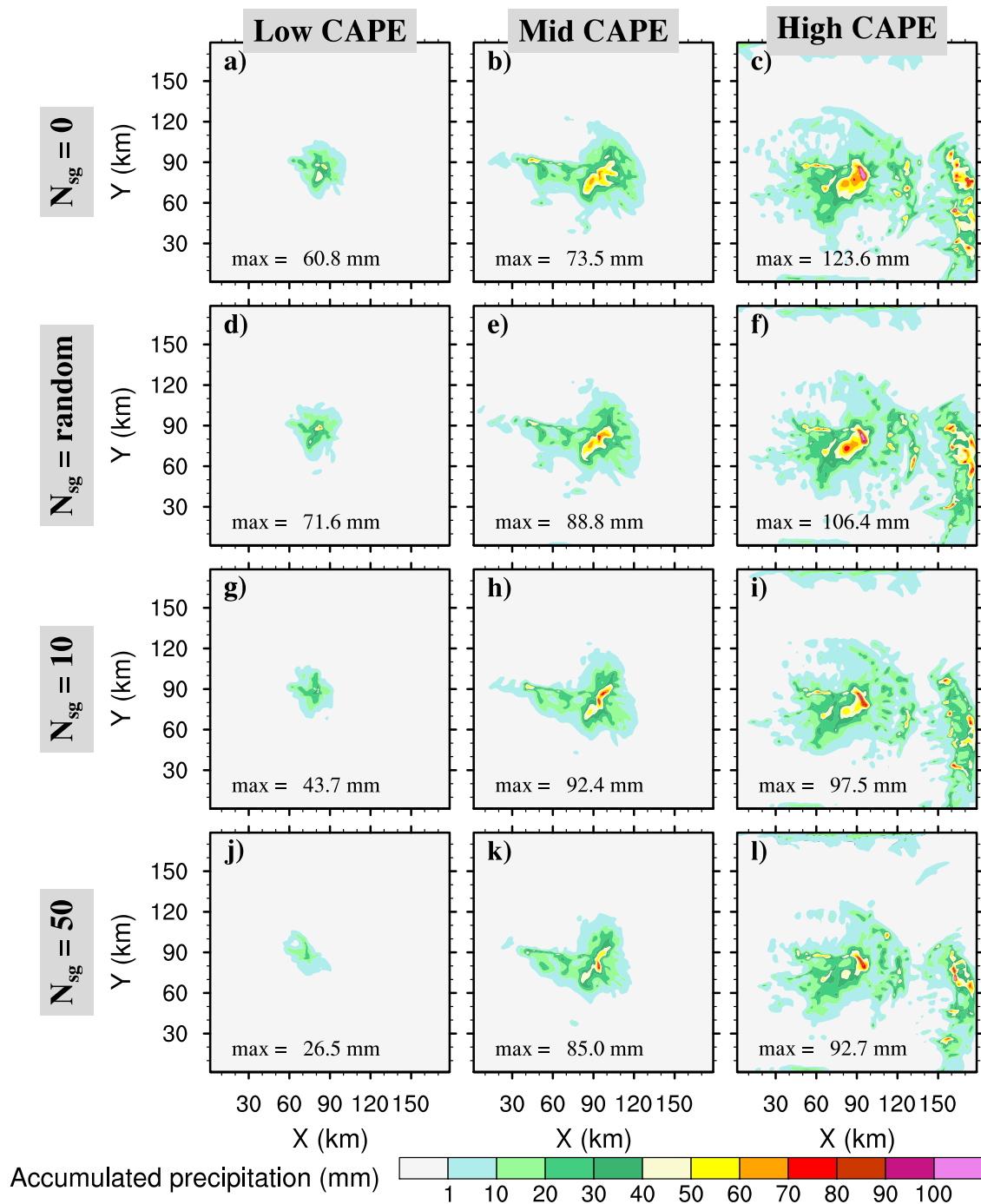


Figure 17. As in fig. 16, but for the 4-h accumulated precipitation of the WK84 simulations. The peak value (max in mm) corresponds to the peak value of precipitation of the main convective clouds in the centre of the simulation domain.

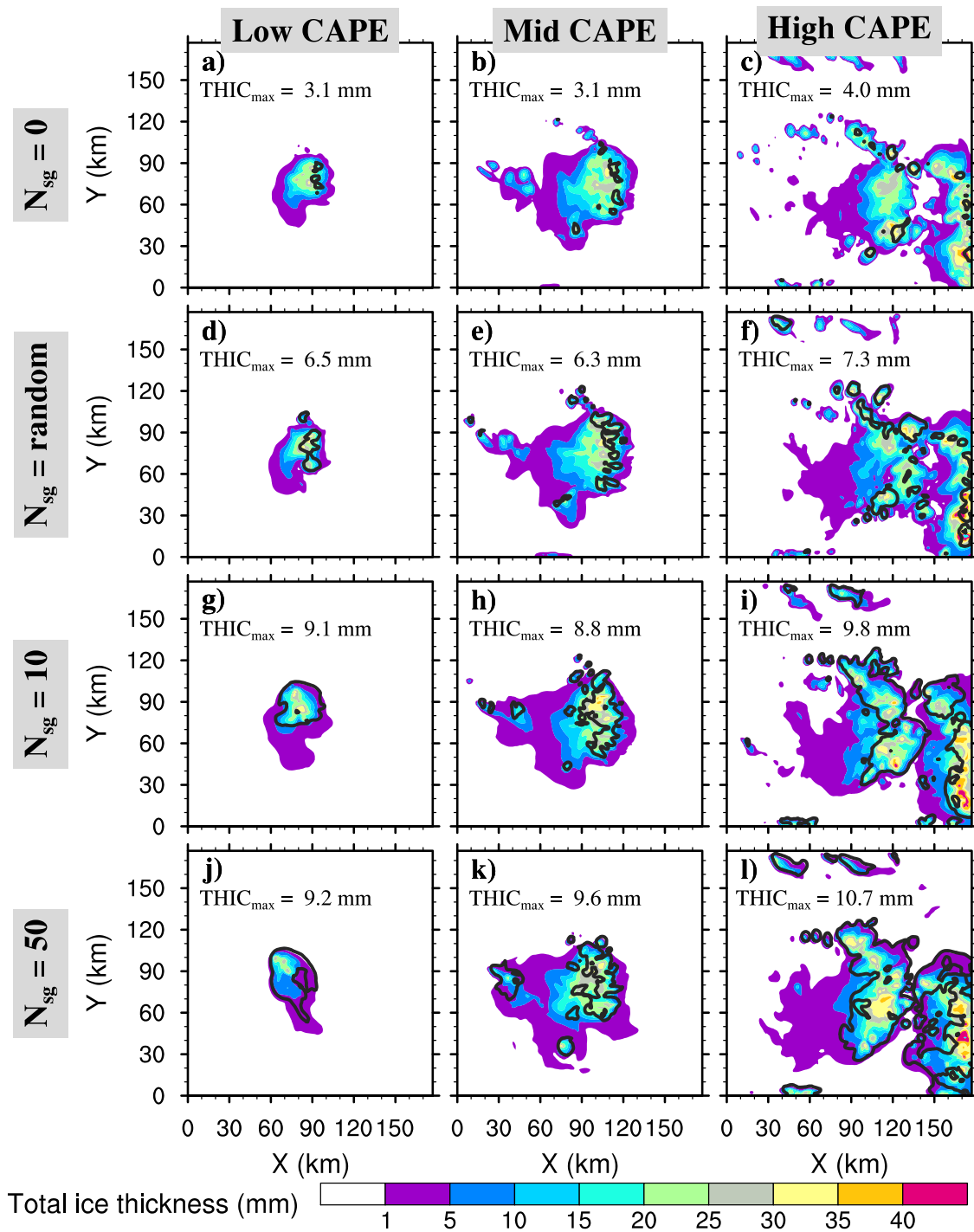


Figure 18. As in fig. 16, but for the total ice thickness in mm after 4 hours of the WK84 simulations. The additional isocontours are the small ice thickness component (THIC) taken at 1 mm. The peak value of THIC ( $THIC_{max}$  is given in mm).

## Responses to Referee #01

“A representation of the collisional ice break-up process in the two-moment scheme LIMA v1.0 of Meso-NH” by Hoarau et al.

### Major comments

*Thank you for including a description of the LIMA scheme and the STERAO case study. These help the coherence of the manuscript. Many, but not all, of my questions have been addressed in the author response, and I have no objection to its publication in GMD. I am still not sure how the parameterization addresses the discrepancy between ice crystal and INP numbers found at mixed-phase conditions, given the highest simulated CIBU contributions at cirrus altitudes. Allowing the process to occur over a wider range of altitudes than in the real atmosphere will certainly affect the results through the vertical latent heating profile and the impact of that heating on dynamics. Some discussion of these considerations could be incorporated.*

Even if the manuscript is amendable, we appreciate the positive feedback of the reviewer. The discrepancy between ice crystal and INP number concentrations is not something new but it was recently exacerbated because secondary production of ice crystals is becoming an open question besides the Hallett-Mossop process just above the freezing level.

We have added a new case (more precisely the Weisman-Klemp cases with varying CAPE) in the manuscript to check how the effects of CIBU could be generalized. Through this case, it is possible to show the growing horizontal extension of the ice clouds and an increase of the mean cloud tops when the number of fragments increases. Interestingly, this suggests that convection develops more when CIBU is very strong because a large excess of small ice crystals leads to heating when supersaturated water vapour deposits on these small crystals. However we do not want to go too much farther until the parameterization of CIBU has been well constrained by data (cloud coverage, precipitation at the ground, etc.).

*In line with this kind of discussion, a visualization of the “upward transport in the convective cells” of ice crystals formed by CIBU would also be appreciated, since from Figure 9, it seems rather that there is a sedimentation loss from these altitudes. The manuscript could still do with some proofreading because the wording is hard to understand in places.*

The ice crystals formed by CIBU would be difficult to isolate because they are mixed with those produced by nucleation and by Hallett-Mossop. For instance, a major sink of cloud ice, the transfer to the snow-aggregate category, depends on the deposition rate of big crystals of the total cloud ice crystal size distribution. However it is clearly beyond our purpose to propose, first, a parameterisation of CIBU and then to illustrate some consequences of the inclusion of CIBU in 3D cloud resolved simulations.

### Specific comments

*Line 27 – “The CIBU process was overlooked in cloud physics. So to our knowledge a contribution of CIBU is never accounted for in the vast majority of the currently used microphysics schemes.” This is still poorly worded. Can you simply say: “In contrast to the Hallett-Mossop process, the majority of microphysics schemes do not include the CIBU process.”*

The final wording is now:

*“However, intriguingly and in contrast to the Hallett-Mossop (hereafter H-M) ice multiplication mechanism<sup>1</sup> (Hallett and Mossop, 1974), the vast majority of microphysics schemes do not include the CIBU process.”*

*Line 29-30 – “Yet, even without absolutely incontestable clues, still missing even in recently published cloud data records” I would remove this, as it is superfluous.*

We agree.

*Line 41 – It does not make sense to motivate the work by a discrepancy between IWC and INP number. It is a discrepancy between ice crystal number concentration and INP number.*

This was a mistake, ‘ice water contents’ has been replaced by ‘ice water concentrations’.

*Lines 63-64 – It is not clear what an “asymmetric collision” is. I would still prefer “mass loss” to “erosion”.*

“asymmetric” has been removed. Also we have replaced “erosion” by “mass loss”.

*Line 72 – Remove one “ice” from ice number concentration.*

Done.

*Line 84 – “Collisions” is a preferable term to “shocks” that are generally electrostatic phenomena (and the latter happens due to ice during lightning formation so the potential for confusion is particularly high).*

Done.

*Lines 113-114 – I am still not clear from the author response how both  $D_{s,max}$  and  $D_{g,min}$  are chosen based on a single criterion for relative terminal velocity. If it is just a matter of choosing round numbers because there are no other constraints, this should be stated explicitly.*

It is implicitly true that we are taking round numbers for  $D_{s,max}$  and  $D_{g,min}$ . This is now explicitly stated in the text.

“The choice of round numbers for  $D_{s,max}$  and  $D_{g,min}$  is above all dictated by ...”

*Line 138 – Unless I missed it, you do not mention which nucleation scheme is used. This should be included to know if the nucleation tendencies in Figure 13 should be on the high or low side.*

The heterogeneous ice nucleation scheme is based on Phillips et al. (2008 and 2013). It is adapted to the LIMA scheme as described in Vié et al. (2016) with an integration over the IFN size distribution. We consider ice nucleation by deposition, when the ice nuclei are totally insoluble, and ice nucleation by immersion, for partially soluble ice nuclei, separately. In our case, the homogeneous freezing of the cloud droplets is very low.

We have completed the original sentence (line 140-142) for clarification:

“The ice phase is more complex as we consider the nucleation by deposition on insoluble IFN (black carbon and dust) and the nucleation by immersion (glaciation of tagged droplets because they are formed on partially soluble CCN, containing an insoluble core).”

In Fig. 13, HIND (nucleation by deposition) is shown in purple.

*Line 156 – I would still explicitly state “In a 2-moment bulk scheme.”*

There are spectral or bin microphysics schemes with a detailed description of the particle size distributions (PSD) and bulk schemes which assume a mathematical form of the PSD. To us, moments of the PSD imply a bulk scheme. However we have added the word “bulk” into the text.

*Lines 196-198 – “by a multicellular storm” Please add “over land” here. The STERAO case be “very classical” but not all readers will necessarily be familiar with it. I would also say “three 3 K-buoyant bubbles along the horizontal wind direction” if this is what is meant in line 198.*

We agree with the idea of giving more details about the STERAO storm. We have reformulated the description of the case:

“This case is characterized by a multicellular storm which becomes supercellular after 2 hours. The simulations were initialized with the sounding of northeastern Colorado given in Skamarock et al. (2000) and convection was triggered by three 3K-buoyant bubbles aligned along the main diagonal of the X,Y plane in the wind axis.”

We have removed the words “very classical”.

*Line 226 – I do not think “disruptive process” is a clear description. I would just say “From these simulations, inclusion of CIBU can strongly modify surface precipitation when  $N_{sg} > 10.0$  fragments per aggregate-graupel collision.”*

We agree to replace the sentence by the suggestion of the reviewer.

“From these first 3D numerical experiments, inclusion of CIBU can strongly modify surface precipitation when  $N_{sg} > 10.0$  fragments per aggregate-graupel collision.”

*Lines 233-235 – Here again, a direct comparison of ice mass and number metrics does not make sense. Presumably you mean that higher ice crystal concentrations with larger  $N_{sg}$  deplete the supersaturation that would otherwise go to snow-aggregate growth. Please say this instead.*

Yes we have followed the suggestion.

“Basically, intensifying the CIBU process by increasing  $N_{sg}$  leads to higher cloud ice crystal concentrations, which deplete the supersaturation of water vapour that would otherwise contribute to the deposition growth of the snow-aggregates.”

*Line 242 – Why would one expect any change in the graupel mixing ratio at all since, from Lines 178 to 179, “the mass of the graupel is unchanged” in this CIBU parameterization?*

You are right, this is confusing. So we have added a sentence.

“... a reduction of  $r_g$  which clearly stands out at  $z=8,000$  m. The decrease of  $r_g$ , even if graupels are passive colliders for CIBU, is the result of the decrease of  $r_s$  in the growth chain of the precipitating ice. The final result ...”

*Line 257 – Again can you make clear why there should be a reduction in  $r_g$  given that the graupel are acting as “passive colliders” in your parameterization?*

Done, see above.

*Figure 9, author response – I understand that nucleation has a much more important impact on ice number than ice mixing ratio. But here and throughout, a motivation to explain ice mass seems misguided to me. Ice-ice collisional breakup was proposed to explain discrepancies in measured ice number concentrations.*

We fully agree but, besides changing  $N_i$  with CIBU, it is necessary to examine the impact on  $r_i$  as the new small ice crystals pump the excess water vapour, with some consequences for the graupels at the end of the growth chain.

*Around Line 277, author response – I am still unclear about why ice mixing ratio and number concentration peak at different altitudes. In the author response, I am not sure what the “limiting value  $dr_i/dt$ ” means. Can you clarify? There are no min functions in Equations 3 to 5.*

The mass growth of the cloud ice, concerning the CIBU contribution, is computed as the mean mass of the pristine ice crystals (a local value) times the local CIBU tendency,  $\partial N_i/\partial t|_{\text{CIBU}}$  in Eq. 3. So  $\partial r_i/\partial t|_{\text{CIBU}} = (r_i/N_i) \times \partial N_i/\partial t|_{\text{CIBU}}$ . This is justified because CIBU is not associated with a characteristic or specific hump on the small ice crystal size distributions.

However, in any case,  $\partial r_i/\partial t|_{\text{CIBU}}$  must be limited by the mass of colliding individual aggregates given by Eq. 5. This is why we talked of “limiting value of  $\partial r_i/\partial t$ ” in our response. This is clearly described in the text (section 2.3).

*Line 312-314, Figure 13 – I am curious why the Hallett-Mossop on Graupel process peaks around 5 km if the graupel mixing ratio peaks around 9 km. Is the droplet number large enough to compensate for such low graupel mixing ratios?*

Hallett-Mossop needs graupel and cloud droplets (more abundant in the low levels). But, more importantly, this process is efficient in the [-3, -8] range of temperature (and reproduced by a symmetrical triangular function). This explains why Hallett-Mossop peaks around 5 km.

*Line 305, author response and Lines 340-341 – If the INP number is high enough to deplete supersaturation, you have no homogeneous nucleation. I would imagine that is why you see a decrease in  $N_i$  concentration with increasing IFN in Figure 14b.*

Yes we agree that less supersaturation decreases nucleation in Phillips et al.’s (2008 and 2013) papers.

## **Additional references**

Phillips, V. T., DeMott, P. J., and Andronache, C.: An empirical parameterization of heterogeneous ice nucleation for multiple chemical species of aerosol, *J. Atmos. Sci.*, 65, 2757–2783, 2008.

Phillips, V. T., Demott, P. J., Andronache, C., Pratt, K. A., Prather, K. A., Subramanian, R., and Twohy, C.: Improvements to an empirical parameterization of heterogeneous ice nucleation and its comparison with observations, *J. Atmos. Sci.*, 70, 378–409, 2013.

## Responses to Referee #02

“A representation of the collisional ice break-up process in the two-moment scheme LIMA v1.0 of Meso-NH” by Hoarau et al.

*In their revised manuscript, Hoarau et al. have addressed some of my concerns but not all of them. I appreciate that more details about the model setup and microphysics schemes have been added. However, I still see no discussion on the limitations of the experimental setup, no justification for why  $0.1 < N_{sg} < 10$  is a physically plausible range, and no justification for the authors' conclusions that more work needs to be done by the measurement community to further constrain this range. Additionally, I did not find that the authors made a real effort to improve the language and readability of the manuscripts. As it stands, I still can't recommend publication in GMD.*

We thank the referee for his careful review. We hope to have satisfactorily answered to the questions and addressed all the concerns.

The purpose of the work is to show a simple implementation of the Collisional Ice Break-Up (CIBU) process and to study the consequences of this operation in a cloud resolving model. The intensity of the CIBU process depends on the  $N_{sg}$  parameter, that is, the number of ice fragments produced per “snow-graupel” collision. This parameter is crucial and not well known despite a few lab data.

In our application to STERAO, we show that taking  $N_{sg} > 10$  leads to a measurable decrease of the surface precipitation in 3D simulated cloud systems. We add new simulations of supercell storms with a varying CAPE following the technique of Weisman and Klemp (1982). This second series of (WK) experiments confirm that the accumulated precipitation is affected by a strong CIBU efficiency, up to  $N_{sg} = 50$ .

As a result, one can see that is very easy to increase the cloud ice concentration  $N_i$  by several orders of magnitude through a secondary process of ice production like CIBU even if the proposed parameterization of CIBU seems too simplistic or not sufficiently grounded. It is less easy to increase  $N_i$  while not perturbing the surface precipitation too much. So, for these reasons we suggest randomizing  $N_{sg}$  to obtain high values of  $N_i$  very locally.

The last WK simulations show that a rough tuning of CIBU could be achieved by examining the coverage of ice clouds connected with a convective outbreak.

We have revised our conclusions. We no longer suggest limiting the upper range of acceptable values for  $N_{sg}$  to 10 but we encourage other microphysics schemes to include CIBU and to check the consequences of CIBU by simulating deep convective events. This is a useful task because adding a very large number of small ice crystals should have a profound impact on the genesis of precipitation.

This step, i.e. the transfer and the growth of cloud ice to hydrometeor categories, often differs among microphysics schemes.

The readability of the whole manuscript has been very carefully revised by a native English speaker.

### *Major concerns*

#### ***The importance of realizing that results are specific to the experimental setup.***

*I appreciate the efforts of the authors to investigate a range of Nsg values. However, the results haven't been shown to be robust (e.g. generalizable to some degree to more deep convective cases). That is because the experiments weren't conducted for different cases, and perturbations to the initial conditions and other details of the microphysics scheme haven't been carried out. I understand that the authors may not wish to add experiments at this point, but there at least needs to be an emphasis on this being a limitation. The authors did conduct sensitivity tests to the initial concentration of ice freezing nuclei, these may be enough to establish some trend in the impact of CIBU on LIMA, but the authors do not give that part of the study the attention needed to do so.*

In the latest revised version, we have added WK, a deep convective case studied by Weisman and Klemp (1984), to show that, with a varying CAPE, inclusion of CIBU with a variable strength confirms the STERAO results.

We agree that a lot of work is necessary to establish more firmly that collisional ice break up is an important process besides raindrop shattering, for the microphysics of deep convective clouds. The interaction between ice nucleation and ice break-up deserves a more specific study. For instance, a heavy secondary production of ice crystals (here, through CIBU) necessarily perturbs the supersaturation field in the clouds with a possible competition between nucleating IFN and growing ice crystals or ice fragments.

#### ***The authors' conclusion that a range of plausible Nsg has been realized has not been justified.***

*This in part follows from the preceding critique. Only one case has been simulated, very few changes to said case have been carried out which makes it difficult to conclude that this range can be generalized. In addition, I am still not convinced that a conclusion can be drawn based on how small or large the induced perturbation to the storm dynamics and microphysics. The authors may have a good understanding of this, but they still haven't communicated it well. Please revise this point. Write a very clear paragraph or even section explaining to the reader why a perturbation of a particular magnitude must not be exceeded when CIBU is introduced.*

Another case (“WK” sounding) is simulated now and we retrieve the same conclusion of the STERAO case that the production of a high number of ice fragments is deeply perturbing the microphysics state of the clouds with less surface precipitation and an extended ice cloud cover (but when the atmosphere is not too dry in the vicinity of the cloud tops).

We attenuate our previous conclusions that  $N_{sg}$  should not exceed some precise threshold. However, a possible way of doing is also to work on the concept of random process for CIBU to get high values of  $N_i$ , but very locally.

***The conclusion that more measurements are needed to constrain the  $N_{sg}$  range.***

*As the authors note, it is extremely important for a study such as this to guide future measurements. There is some discussion of this in the conclusions, but it's unclear. Please write a clear paragraph or section indicating the kinds of measurements needed based on the results.*

This is a little bit beyond the purpose of a study based on simulations. However and after the “WK” simulations, we reworked the conclusion to suggest that looking at the ice cloud cover may be a way to get a macroscopic adjustment of the  $N_{sg}$  parameter. Anyway, a fundamental need is to redo laboratory experiments in chambers with controlled environment and to get in situ sampling of the ice crystals (formvar replicator) to characterize the alterations of the crystal habits.

***The sensitivity studies are poorly discussed.***

*I understand the desire to write a short paper. We should always strive to write manuscripts in the least wordy way possible. However, this should not come at the expense of poor elaboration on the results of the experiments. It becomes especially frustrating when the reader reaches the interesting section of sensitivity to initial ice nucleating concentrations and is met with a very limited interpretation of what is happening.*

We agree but model results depend also on model set-up here, the initial concentrations and vertical profiles of the CCN and IFN particles. We try to be careful when drawing general conclusions with a limited set of experiments.

The question of the initial concentration of IFN is introduced to check if CIBU is still operating in the case of very low IFN concentrations. This corresponds to a marginal functioning of the LIMA scheme. However the results show that once the ice phase is initiated by ice nucleation (IFN are always indispensable), ice multiplication is possible. The conclusion is that the availability of the IFN, down to  $0.001 \text{ dm}^{-3}$ , seems not a limitation for CIBU in the STERAO case.

***The language remains a limitation.***

*Unfortunately, many statements made by the authors may struggle to be understood by a reader due to deficiencies in language. I had urged the authors to revise this aspect of the manuscript, but very little effort was made.*

We agree and we apologize for that. The new version of the manuscript has been revised in deep.

*Line by line concerns*

*Sec .1. L54-55. "Huge" is not quantitative. Please replace with an actual enhancement factor.*

On the basis of original Fig. 4 of Takahashi et al. (1995), it was difficult to say more than "huge" since the number of fragments lies between approximately 50 and 600. The paper also shows a wide variability of the number of "ejected" ice particles at a given temperature. So it was not possible to be more quantitative, although we risked indicating a value of 400 fragments in the next sentence.

*Sec. 1. L56-57. This sentence is not clear. I'm struggling to understand what "The experiment setup used there was more appropriate to very big" means.*

We have summarized the laboratory experiment by noting that the colliders were "1.8 cm diameter ice sphere(s)". The speed of the grazing collisions was varied to simulate the impact velocity between large and small graupels (4 m/s corresponding to a big particle of ~4 mm).

*Sec. 1 L58-63. There is no need to clarify what the study is not. This series of sentences can be omitted, assuming the authors can clarify what the study entails in the sentences that follow.*

We thought that, because Yano and Phillips's papers (*loc. cit.*) were heavily oriented to the study of the "explosive" nature of ice multiplication by collisional break-up, we would like to be careful by saying that our goal was to implement a simple parameterization of CIBU and then to examine the perturbations brought to the cloud microphysics.

With this way of working we consider that CIBU is a common process that should operate when cloud conditions are met (presence of aggregates and graupels) and no more.

*Sec. 2.1 L88-89. Since the authors haven't introduced what the categories are at this point, they should not expect the reader to understand what "small aggregates covering pristine ice" and "large graupel particles" are. Start by*

*explaining what the categories are, then clearly state which categories are considered for collisional breakup and what size restrictions are applied.*

The reviewer is right, the first sentence of the paragraph has been reworked:  
“In contrast to the work of Yano and Phillips (2011), where large and small graupel particles fuelled the CIBU process, we consider collisions involving two types of precipitating ice here: small ice particles growing by deposition and aggregation (aggregates including dendritic pristine ice crystals with a size  $>150 \mu\text{m}$ ) and big, massive graupel particles growing by riming.”

*Sec. 2.1 L95. “Symbolic” is not necessary here.*

Right. We have replaced it by “general” because, more precisely, the “ $n$ ” represent particle size distributions. Then, at the beginning of Section 2.3, we specify that “ $N$ ” is a total number concentration (zeroth moment of  $n$ ).

*Sec. 2.1 L99. “Simplest” is not necessary here. The writers should say “an expression for  $\alpha$  which \*” where \* would state what the assumptions behind the expression are.*

We have followed the suggestion. The sentence is now:

“An expression for  $\alpha$ , which does not include thermal and mechanical energy effects, is”

*Sec. 2.1 L125-140. I still don’t understand this explanation of  $N_{sg}$  based on previous work and how it ties to this study.*

Well, we tried to review the studies done around  $N_{sg}$  estimates. This critical parameter is a constant or the realization of a random process or it is modelled as in Vardiman (1978) and Phillips et al. (2017). So our purpose was to argue for an upper limit  $N_{sg\_max}$  (here 50) in order to perform simulations for  $0 < N_{sg} < N_{sg\_max}$  to explore the perturbations brought to the microphysics. In any case,  $N_{sg}$  is a number, not the output of a parameterization.

*Sec. 3.1. This is the section where a better job can be done to explain to the reader why a plausible range of  $N_{sg}$  can be concluded.*

Following the suggestion of Rev 1, a sentence has been reworked in this section. Note that, in the last revised version of the manuscript, we added WK cases showing some similarities with STERAO, i.e. a reduction of the precipitation peak value and/or a reduction of the precipitation area.

*Sec. 3.2 L267-268. “rain is mostly fed by melting of graupel particles”. The authors don’t show  $r_r$  production rates from autoconversion vs. melting. Thus, this statement isn’t justified. Consider rewording to something more suggestive.*

The decrease of the  $r_r$  profiles in Fig. 8 is barely visible so we have removed the sentence.

*Sec. 3.2 L266. Avoid using “clearly”.*

Done.

*Sec. 3.3 L276-279. This sentence is not clear. You are stating what the main processes are but simultaneously talking about how AGGS and CFRZ are changing? Please reword.*

We have rewritten the paragraph:

“As expected, the tendencies of  $r_i$  (Fig. 9a-c) are the most affected by the CIBU process. The main processes standing out in Fig. 9a, when CIBU is not activated, are CEDS (Deposition-Sublimation), essentially a gain term and AGGS (Aggregation), the main loss of  $r_i$  by aggregation at a rate of  $0.5 \times 10^{-3} \text{ gkg}^{-1}\text{s}^{-1}$ . The loss of  $r_i$  by CFRZ (Drop Freezing by Contact) makes a moderate contribution as some raindrops are present in the glaciated part of the storm. Above  $z=10,000 \text{ m}$ , the net loss of  $r_i$  (AGGS and SEDI, the cloud ice sedimentation) is balanced by the convective vertical transport (not shown). When  $N_{sg} = \text{RANDOM}$ , the  $r_i$  tendencies are amplified even with a modest contribution of  $\sim 0.2 \times 10^{-3} \text{ gkg}^{-1}\text{s}^{-1}$  for CIBU itself. The growth of AGGS, which doubles at 10 km height, is caused by CIBU and by an increase in the convection because SEDI (a loss) is amplified in response to an increase of  $r_i$  in the upper levels. The CFRZ contribution is also increased. The last case, with  $N_{sg} = 10$  (Fig. 9c) confirms a further increase of the rates except for CFRZ, interpreted here as a lack of raindrops.”

*Sec. 3.4 L300-319. This is too dense. Please expand this explanation.*

The whole paragraph has been rewritten:

“The next point examines the behaviour of the cloud ice number concentration as a function of the strength of CIBU after 4 hours of simulation. Figure 12 shows that the altitude of the  $N_i$  peak value decreases when  $N_{sg}$  increases. In the absence of CIBU ( $N_{sg} = 0$ ), the source of  $N_i$  is the heterogeneous nucleation processes on insoluble IFN and on coated IFN (nucleation by immersion) which are more efficient at low temperature. Nucleation on IFN provides a mean peak value of  $N_i = 400 \text{ kg}^{-1}$  at  $z = 11,500 \text{ m}$ . In contrast, the  $N_{sg} = 10$  case (here scaled by a factor 0.1 for plotting reasons) keeps the trace of an explosive production of

cloud ice concentration,  $N_i = 7,250 \text{ kg}^{-1}$ , due to CIBU. The altitude of the maximum of  $N_i$  in this case ( $z = 10,000 \text{ m}$ ) is consistent with the location of the maximum value of the  $r_s \times r_g$  product (see Fig. 8). The "RANDOM" simulation produces  $N_i = 1100 \text{ kg}^{-1}$  at  $z = 11,000 \text{ m}$ , a number concentration which is similar to that found for the  $N_{sg} = 2$  case. Table 2 reports the peak amplitude of the  $N_i$  profiles as a function of  $N_{sg}$  but after 3 hours of simulation, when the CIBU rate is strongly dominant. Additional cases were run to cover  $0.1 < N_{sg} < 50$  with a logarithmic progression above  $N_{sg} = 1.0$ . A CIBU enhancement factor,  $\text{CIBU}_{\text{ef}}$ , is computed as  $N_i(N_{sg}) / N_i(N_{sg} = 0) - 1$ , as  $N_i(N_{sg} = 0)$  stands for a baseline not affected by CIBU. The results show that the growth of  $N_i$  is fast when  $N_{sg}$  reaches  $\sim 5$  ( $\text{CIBU}_{\text{ef}}$  switches from 135 % to 913 % when  $N_{sg}$  moves from 2 to 5). Taking  $N_{sg} = 50$  leads to an extremely high peak value of  $N_i$ ."

*Sec. 3.4 L306-307. Please clarify that the  $N_i$  achieved when not considering CIBU is not the actual concentration of ice nucleating particles, but the resultant concentration of ice. This is an important distinction.*

We don't understand this remark. We consider several sources of IFN on the one hand and a single concentration of cloud ice on the other hand. The budget of the  $N_{\text{IFN}}$  is independent of the budget of  $N_i$  because the IFN are also state variables in LIMA. Adding or ignoring CIBU doesn't change the situation.

*Sec. 3.4 L320-321. "Temporal integration" is too wordy. Consider using something simpler like "time integrated" if that's what you mean here.*

We have adopted "time integration".

*Sec. 3.4 L325-327. Reword this please. "In the case of water supercooling" is not clear.*

In the LIMA scheme, the Hallett-Mossop process operates with the riming of the graupel (HMG) and also during the riming of the snow-aggregates category (HMS). The heavy riming of the snow-aggregate particles is a source term for the graupel, so Hallett-Mossop should operate there. The sentence has been reworded as follows:

**"Here, we consider that H-M also operates for the snow-aggregates because this category of ice includes lightly rimed particles that can rime further to form graupel particles."**

*Sec. 3.5 L351-353. Why is it difficult to interpret? The results seem clear here. I highly urge expanding this section in such a way to discuss the sensitivity to ice nucleating particle concentrations without CIBU first (beyond two brief sentences) then move on to the case with CIBU.*

We found it was difficult to interpret because there is no clear trend in the “no CIBU” case of Fig. 14b to understand the sensitivity of  $N_i$  to  $N_{IFN}$ . We could expect  $N_i$  to grow in proportion to  $N_{IFN}$  but this is not the case. A possible reason is that we are dealing with mean vertical profiles and also, after 4 hours of model integration, the simulations may start to diverge and cease to be comparable. Also the supersaturation field of water vapour is not tracked during the simulations to see if it plays a role. It is true, however, that this is a point to investigate more in the future.

*Concerns not addressed in the first round of revision*

*Below is a list of comments I wrote in the first round that I believe were not properly addressed.*

*Sec. 2.1: Please justify the choice of a temperature independent  $N_{sg}$  here. For example, Sullivan et al. (2017) use an  $N_{sg}$  that is temperature dependent.*

Sullivan et al. (2017) were inspired by the results of Takahashi et al. (1995), in which we have little confidence for many reasons: 1/ there is a large spread of the data around  $-15^{\circ}\text{C}$  and  $-20^{\circ}\text{C}$  (see above) so it is questionable how a temperature-dependent formula could be adjusted (by eye, we guess), 2/ the number of fragments per collision is at least ten times more than what was carefully observed by Vardiman (1978) with natural crystals, 3/ the laboratory apparatus of Takahashi does not simulate the break-up of, for instance, radiating dendritic crystals; it is appropriate to the study of collisions between very big, artificially grown, graupels, which do not break up (it seems that it is more the protuberances on the rough surface of the graupels that are ejected and produce the “fragments”).

In our work, we put forward the size distribution properties of the colliders to select the range where CIBU should operate, in order to integrate over it. This is in contrast with Sullivan et al. (2017) who were working with less realistic, monodispersed particles. Even if there is a temperature dependence of the CIBU efficiency, we believe that the most important features of CIBU are the particle size dependence and the cloud conditions leading to the occurrence of aggregates and graupels. We also think that additional laboratory experiments are truly necessary to confirm any thermal effect on CIBU.

*Sec. 3.1. L199-202: This statement is unjustified. As emphasized in the preceding comment, realism of a specific  $N_{sg}$  range has not been established, therefore the writers' conclusion on the choice of  $N_0$  by Yano and Phillips (2011) being unrealistic is not justified. Also there aren't enough details about the cited study to make a meaningful comparison here.*

We don't claim that the choice of  $N_0=50$  by Yano and Phillips (2011) is unrealistic. Our results suggest that taking  $N_{sg}$  as high as 50 leads to very high  $N_i$  concentrations (well, that's fine!) but taking  $N_{sg}=50$  also strongly decreases the surface precipitation in some cases and so this is a little bit annoying because one purpose of microphysics schemes is to simulate accurate surface precipitation. Up to now, after Yano and Phillips (2011) or Sullivan et al. (2017, 2018), no experiment with a complete microphysics scheme has been performed in 3D simulations to check the consequences of a huge increase in  $N_i$ .

*Sec. 3.4. L280: Why is HIND more efficient here? Is it because the air becomes subsaturated with respect to liquid water? Why about homogenous ice nucleation? What are HMG and HMS*

If you are curious to understand why HIND is more efficient at 14 km when  $N_{sg}=\text{RANDOM}$  than when  $N_{sg}=0$ , we have no short and solid explanation to offer. Basically HIND is more efficient when the concentration of IFN is increased or when the supersaturation of water vapour over ice is large but, here, there is no obvious connection with the increase of  $N_i$  due to CIBU. The point you raised, interaction between nucleation and CIBU, deserves more investigations with specific diagnostics but it is well beyond the topic of the study.

The homogenous ice nucleation is not a very important source of cloud ice in our simulations. This is what we found.

The meaning of HMG and HMS were given in Table 3, they are source terms for  $N_i$ .